Drosophila host defense mechanisms against filamentous fungal pathogens with diverse lifestyles

Guiqing Liu[1,2*], Yao Tian[1], Mark Austin Hanson[3], Jun Li[2], Bruno Lemaitre[1*]

1 Global Health Institute, School of Life Science, École Polytechnique Fédérale de Lausanne (EPFL), Lausanne, Switzerland.

2 Guangdong Key Laboratory of Animal Conservation and Resource Utilization, Institute of Zoology, Guangdong Academy of Sciences, Guangzhou, China.

3 Centre for Ecology and Conservation, Faculty of Environment, Science, and Economy, University of Exeter, Penryn, United Kingdom.

*Correspondence

guiqing.liu@foxmail.com, bruno.lemaitre@epfl.ch

Abstract

Entomopathogenic fungi serve as powerful regulators of insect populations in nature. The infection outcome depends on the complex interplay between insect immune defenses and fungal adaptive strategies. However, how host immune effectors contribute to resist fungi with different ecological strategies remains incompletely understood. In this study, we employ *Drosophila melanogaster* as a genetically tractable model to dissect immune defenses against diverse fungal pathogens. Our study uncovers that the Toll pathway is the key determinant of immunity against all species tested regardless of their ecological strategy, primarily through resistance mechanisms that limit fungal proliferation. In addition, melanization, but not phagocytosis or the Imd pathway, also has a role in limiting fungal entry and proliferation. Additionally, we show that fungal protease detection by Persephone has a quantitatively more critical role than the glucan sensor GNBP3 in the activation of the Toll pathway upon fungal infection. Our study also reveals that the fly-specific obligate fungus *Entomophthora muscae* employs a vegetative development strategy, protoplasts, to hide from the host immune response. These findings reveal that Drosophila immune mechanisms effectively defend against a broad range of fungal pathogens with various ecological

lifestyles, while highlighting striking adaptations to overcome these defenses in highly specialized fungal pathogens.

Keywords: host-pathogen interactions, fungal pathogens, innate immunity, *Drosophila*

Introduction

Fungal infections are widespread in nature and exert a profound impact across a wide range of organisms, including agriculturally significant plants, insects, and humans (Brown, 2023; Dean et al., 2012; Wang and Wang, 2017). Interactions between fungal pathogens and their hosts are highly dynamic and intricate. This complexity arises from the vast evolutionary diversity of fungal pathogens and the ever-changing host microenvironments that influence their infection (Brown, 2023; Dean et al., 2012; Wang and Wang, 2017). An enhanced understanding of host-fungus interactions could lead to the development of more effective strategies for managing fungal infections of global importance in agriculture, public health or environmental management (Casalini et al., 2024; Rommelaere et al., 2025).

Fungal pathogens have evolved within different niches. Saprotrophic fungi such as *Cryptococcus neoformans* and *Aspergillus fumigatus* primarily inhabit the environment but have evolved independent mechanisms that facilitate animal infections (Morelli et al., 2021; Ristow et al., 2023). In contrast, other fungal pathogens, including *Candida albicans* and entomopathogenic fungi such as *Metarhizium* and *Beauveria* species, have co-evolved with their hosts (Brown, 2023; Hu et al., 2014). Some, under strong selection to exploit their hosts for survival, have even become obligate pathogens as seen in *Entomophthora* and *Ophiocordyceps* species (Ballou et al., 2016; De Fine Licht et al., 2017; Liu et al., 2019; Wang and Wang, 2017). Unlike human-pathogenic fungi, entomopathogenic fungi can hardly grow or even survive at 37°C (Siscar-Lewin et al., 2022). The genus *Metarhizium* includes generalist species capable of infecting hundreds of insect species across various orders (e.g. *M. robertsii*, formerly classified as *M. anisopliae*) and specialist species with a narrow host range (e.g. *M. acrium* and *M. rileyi*). Comparative genomic analyses suggest that generalist species evolved from specialists by broadening their repertoire of virulence factors (Gao et al., 2011; Hu et al., 2014). Intriguingly, some specialists such as *E. muscae* and *O. unilateralis*

manipulate host behavior. They prompt infected insects to climb to elevated positions, affix themselves with their proboscides, and then splay their wings before dying, thereby facilitating fungal spore dissemination (Elya et al., 2018; Hughes et al., 2011).

Entomopathogenic fungi play a crucial role in regulating insect populations in natural ecosystems. Among them, the genetics and infection biology of *Metarhizium* and *Beauveria* species have been extensively studied and several strains have been developed as environmentally sustainable mycoinsecticides (Wang and Wang, 2017). Unlike bacterial and viral pathogens, which primarily utilize oral or respiratory routes, entomopathogenic fungi primarily infect insects through direct penetration of the cuticle and proliferate within the hemolymph. As a result, they must overcome multiple defenses, including cuticular barriers and both localized and systemic immune responses (Levitin and Whiteway, 2008; Mpamhanga and Kounatidis, 2024; Westlake et al., 2024).

On the pathogen side of host-pathogen interactions, entomopathogenic fungi have evolved various virulence factors to overcome or evade host defense (Cen et al., 2017; Ma et al., 2024; Qu and Wang, 2018; Tang et al., 2025; Valero-Jiménez et al., 2016; Wang et al., 2023). Comparative genomic studies indicate that generalist fungi tend to have an expanded repertoire of diverse protein families compared to specialist fungi, including cuticle-degrading proteins (proteases, carbohydrate esterase) and pathogen-host interaction proteins (Hu et al., 2014; Shang et al., 2016; Wichadakul et al., 2015). However, the pathogenic mechanisms of less-studied fungi, such as *M. rileyi* and *E. muscae*, as well as the host defense responses they elicit, remain largely unexplored (Boucias et al., 2016; Elya and De Fine Licht, 2021).

The fruit fly *Drosophila melanogaster* serves as a powerful model organism for investigating multiple defense mechanisms against fungal infections (Levitin and Whiteway, 2008; Mpamhanga and Kounatidis, 2024; Westlake et al., 2024). A range of immune receptors detect microbial molecules and damage-associated signals, triggering key immune responses such as the Imd and Toll pathways, phagocytosis and melanization. The Toll and Imd pathways coordinate the production of immune effectors by the fat body during systemic infection (De Gregorio, 2002; Rommelaere et al., 2024; Uttenweiler-Joseph et al., 1998; Valanne et al., 2011; Westlake et al., 2024).

The Imd pathway controls the production of antibacterial peptide (e.g. Diptericin, Cecropin) and is critical to resist infection by Gram-negative bacteria (Carboni et al., 2022; Hanson et al., 2019). The Toll signaling pathway is critical to resist fungal infection and infection with Gram positive bacteria (Lemaitre et al., 1996; Ryckebusch et al., 2025). It can be activated by two mechanisms: if a key fungal cell wall component, β-1,3-glucan, binds to the secreted pattern-recognition receptor GNBP3, or if fungal proteases activate a complex extracellular cascade of serine proteases, the Toll-PO cascade. Both mechanisms converge to the activating cleavage of the Toll ligand Spätzle (Spz) (El Chamy et al., 2008; Gottar et al., 2006; Westlake et al., 2024). Binding of Spz to the Toll receptor initiates an intracellular cascade leading to the production of a battery of host defense peptides (Weber et al., 2003). Among them, genetic and *in vitro* studies have revealed the role of Drosomycin, Metchnikowin, Bomanins, Daisho and Baramicin to combat fungal infection (Clemmons et al., 2015; Cohen et al., 2020; Fehlbaum et al., 1994; Hanson et al., 2021; Levashina et al., 1995). These host defense peptides can function additively or synergistically to combat pathogens, but they can also display high specificity toward a pathogens (Hanson, 2024; Lazzaro et al., 2020). The Toll-PO cascade also activates the melanization reaction. It leads to the maturation of ProPhenoloxidases (PPO) into Phenoloxidases (PO) that produce melanin and reactive oxygen species with antimicrobial activity (Dudzic et al., 2019; Shan et al., 2023; Westlake et al., 2024). The melanization reaction and phagocytosis have been shown to contribute to surviving infection, including by fungi (Binggeli et al., 2014; Feldman et al., 2019; Lohse and Johnson, 2008; Quintin et al., 2013).

Most research on entomopathogenic fungi have focused on a few model species or genera, leaving the full extent of their diversity largely unexplored. Consequently, the roles of immune pathways and effectors in mediating host defense against different types of fungi remain poorly understood. In this study, we use *D. melanogaster* to systematically assess the roles of immune modules, pathways, and immune effectors in resisting fungal infections with varying lifestyles. By employing genetically engineered flies with single and multiple mutations in immune genes, we aim to determine: (i) which immune pathways are crucial and whether the same pathways are used against different fungal species, (ii) the relative importance of immune modules depending on

124 the infection route, (iii) whether immune pathways function independently or
125 synergistically to combat different fungi, and (iv) how antifungal peptides contribute
126 individually or collectively to host defense against fungal infections.
127
128 **Results**
129 **Fungal strains, modes of infection and immune deficient mutants**
130 We aimed to determine whether differences in *Drosophila* antifungal defense could
131 be revealed by using fungal pathogens with distinct lifestyles. We selected five fungal
132 species: *Aspergillus fumigatus*, *Beauveria bassiana*, *Metarhizium anisopliae*,
133 *Metarhizium rileyi*, and *Entomophthora muscae*. *A. fumigatus* is an opportunistic
134 pathogen with limited ability to penetrate the insect cuticle, yet it is pathogenic when
135 introduced systemically (Lemaitre et al., 1996). *B. bassiana*, *M. anisopliae*, *M. rileyi,*
136 and *E. muscae* are entomopathogenic fungi capable of infecting insects through the
137 cuticle (Elya et al., 2018; Wang and Wang, 2017). While *B. bassiana* and *M. anisopliae*
138 have broad host ranges, *M. rileyi* predominantly infects noctuid moths with a more
139 restricted host range (Boucias et al., 2016) and *E. muscae* is a fly-specific obligate
140 pathogen (Edwards and De Fine Licht, 2024).
141 Spores (conidia) from *A. fumigatus, B. bassiana*, *M. anisopliae* and *M. rileyi,* can be
142 produced *in vitro*, allowing us to use two infection methods: natural (topical) infection
143 via immersion of flies in a spore suspension, and systemic infection by direct pricking
144 with a needle dipped in the spore solution. In contrast, *E. muscae* spores cannot be
145 cultured outside its host. For this species, natural infections were initiated by spore
146 shower from cadavers of previously infected individuals as described previously
147 (Edwards and De Fine Licht, 2024; Elya et al., 2018) and protoplasts, which can be
148 grown *in vitro*, were used for injections. Fly stocks were maintained at 25°C, but
149 infections were carried out at 29°C for *A. fumigatus*, *B. bassian*a, *M. anisopliae*, and *M.*
150 *rileyi,* and 21°C for *E. muscae*. The immune pathway mutants and antimicrobial
151 peptide-deficient strains used in this study have been described previously (Hanson et
152 al., 2019; Ryckebusch et al., 2025). Most mutations were isogenized in w^{1118} DrosDel
153 background by seven rounds of successive backcrosses (referred to as "iso"), although
154 some non-isogenized mutants were also included in this study (see full list of genotypes

155 in Table S1).

156

157 **Toll and melanization contribute to surviving fungal natural infections**

158 Survival analysis upon topical natural infection with the five fungi were performed
159 with male w^{1118} *Drosdel flies* (hereafter wild-type flies) and flies specifically deficient
160 for Toll (spätzle, spz^{rm7}), Imd (Relish, Rel^{E20}), phagocytosis ($NimC1^{1}$; $Eater^{1}$) and
161 melanization ($PPO1^{\Delta}$, $PPO2^{\Delta}$), as well as compound mutant flies simultaneously
162 lacking these four modules ($Hayan\text{-}psh^{Def}$; $NimC1^{1}$; $eater^{1}$, Rel^{E20} hereafter named
163 *ΔIPTM* for *ΔIMD, ΔTOLL, ΔPhag, ΔMel*) (Ryckebusch et al., 2025). Survival upon
164 natural infection with these five fungal pathogens reveals the major contribution of the
165 Toll pathway, and to a lesser extent melanization to host defense, while deficiency in
166 IMD and Phagocytosis have no significant effect (Figs. 1A-E). The susceptibility of
167 spz^{rm7} flies was similar to that of *ΔIPTM* flies lacking all four immune modules
168 indicating that Toll is by far the most important pathway to resist all the tested fungi
169 (Table S2). However, *ΔIPTM* flies were more susceptible than spz^{rm7} flies to *A.*
170 *fumigatus,* but this likely reflects the already short lifespan of *ΔIPTM* flies (Fig. 1F), as
171 natural infection with *A. fumigatus* did not cause a strong reduction in lifespan
172 (Ryckebusch et al., 2025). Consistent with the findings in males, a similar role of the
173 Toll pathway and melanization in resisting fungal infection was also observed in
174 females, though with a lesser role for melanization in defense against *B. bassiana* in
175 females (Figs. S1A-E).

176 The four entomopathogenic fungi were more pathogenic to *Drosophila* than the
177 opportunistic pathogen *A. fumigatus* (Figs. 1A- E), reflecting their ability to naturally
178 infect flies. Although *E. muscae* is a specialist fungus that exclusively parasitizes flies,
179 it displayed the same level of pathogenicity as generalist entomopathogenic fungi *B.*
180 *bassiana* and *M. anisopliae*, and the parasitic noctuid specialist *M. rileyi* to spz^{rm7} flies
181 (Compare 1E to Figs. 1A-C). We estimate the quantity of spores released from twenty
182 cadavers for 24 h infection to be around 4.3×10^{3} (Fig. S1F), a much lower spore
183 concentration than the ones used for natural infection with the other four fungi.

184 Collectively, our study reveals that the Toll pathway is the main host defense
185 mechanism upon natural infection with the five fungal species. Beyond the Toll

186 pathway, melanization but not the Imd pathway or phagocytosis plays an important role.
187 Finally, our study reveals the high pathogenicity of *E. muscae* to *Drosophila*.
188
189 **Reduced role of melanization in resisting fungal infection upon septic injury**
190 Injuries allow microbes to bypass the mechanical barrier normally presented by the
191 cuticle and to directly access the nutrient-rich hemolymph. We therefore analyzed the
192 role of the four immune modules in resisting fungal pathogens using a septic injury
193 mode of infection. It should be noted that $PPO1^{\Delta}$, $PPO2^{\Delta}$ flies showed a reduced
194 capacity to survive wounding caused by a clean injury compared with wild-type w^{1118}
195 flies (Fig. 2F) (Binggeli et al., 2014). Survival upon septic infection with spores of *B.*
196 *bassiana*, *M. anisopliae*, *M. rileyi* or *A. fumigatus* revealed faster kinetics of killing as
197 expected from the direct mode of infection that bypasses the crossing of the cuticle.
198 Consistent with the observations done using a natural mode of infection, the Toll
199 pathway was the most effective module in resisting infection by *B. bassiana*, *M.*
200 *anisopliae*, *M. rileyi* and *A. fumigatus*. Interestingly, the contribution of melanization
201 was less marked upon systemic infection compared to natural infection (compare Figs.
202 2A-D to Figs 1A-D). These results suggest that melanization has a key role early in the
203 natural infection process, possibly by inhibiting fungi at the entry sites through the
204 deposition of melanin. Unexpectedly, we observed that Rel^{E20} flies were highly
205 susceptible to *A. fumigatus* upon septic infection (Fig. 2D, Table S3), but not by natural
206 infection (Fig. 1D, Table S2). This points to a role of the humoral Imd pathway against
207 this fungus that becomes important only if the fungus can breach the cuticle.
208 To analyze the host defense against *E. muscae* upon systemic infection, we injected
209 protoplasts in wild-type and immune deficient flies. Faster killing by *E. muscae* was
210 observed when injected with higher concentration of protoplasts (Fig. S2F), which
211 indicates that injection of protoplasts is a valid method to initiate infection in flies.
212 Intriguingly, flies deficient for each of the four main immune modules showed similar
213 susceptibility to the wild-type flies after injection with *E. muscae* protoplasts. Although
214 *ΔIPTM* flies display a significantly increased susceptibility upon injection with *E.*
215 *musca* protoplasts (Fig. 2E), the difference between *ΔITPM* flies injected with *E.*
216 *muscae* protoplasts and clean injury was not significant (Fig. 2F, Table S3), indicating

217 this difference rather reflects the baseline response of *⊿ITPM* flies to injury. Similar
218 findings were consistently observed in females (Figs. 2A-E).
219 We conclude that the mode of infection alters the importance and involvement of
220 different immune modules. Natural infection by depositing spores on the cuticle
221 requires the melanization response to some extent, while direct injection of spores
222 bypasses this melanization-mediated defense. On the other hand, the humoral Imd
223 pathway plays little to no role in defense against natural infection, but an important role
224 can be revealed specifically upon *A. fumigatus* systemic infection. We also observed
225 that injection of *E. muscae* protoplasts kills immune mutant and wild-type flies with
226 similar kinetics, despite immunity being involved in defense against natural infection.
227
228 **Natural infection with *E. muscae* barely induces the Toll pathway**
229 Having revealed its contribution to combat infection with the five fungi, we next
230 monitored the activity of the Toll pathway during the natural infection using the
231 *Drosomycin* (*Drs*) as a read-out, a Toll-regulated gene coding for an antifungal peptide.
232 Natural infection with the *B. bassiana* and *M. anisopliae* triggered a relatively strong
233 expression of the Toll pathway, representing about 20-30% of the level observed 24 h
234 after systemic injury with the model, Toll-eliciting bacterium *M. luteus* (Figs. 3A-B
235 compared to 3F). Natural infection with *M. rileyi* triggers a significant Toll pathway
236 activity although only at the time point of 120 h, suggesting a delayed activation (Fig.
237 3C). *A. fumigatus* did not trigger the Toll pathway within the timeframe upon natural
238 infection, where if anything, *Drs* levels were depressed (Fig. 3D). Collectively, the level
239 of induction of the Toll pathway correlates with the level of pathogenicity using the
240 natural infection mode with *M. anisopliae>B. bassiana>M. rileyi >A. fumigatus*. In
241 sharp contrast, *E. muscae*, despite being very pathogenic to flies, triggers a low
242 induction of *Drs* expression and this upregulation of *Drs* was observed only at the 24 h
243 after infection (Fig. 3E). Expression of another Toll pathway read-out, the Bomanin
244 *BomBc3*, exhibited similar expression to that of *Drs* (Figs. S3A-E). Natural infection
245 of flies carrying the *Drosomycin-GFP* (*Drs-GFP*) reporter (Ferrandon, 1998) also
246 confirmed that *B. bassiana* induced a much strong expression of the Toll pathway
247 compared to *E. muscae* (Fig. 3G). We conclude that natural infection with *E. muscae*

either fails to activate the Toll pathway or suppresses it.

To distinguish between these two alternatives, we compared the Toll pathway activity of unchallenged flies and flies 48 h after natural infection with *E. muscae* upon septic injury with the Gram-positive bacterium *M. luteus,* a strong inducer of the Toll pathway. We found that 24 h post-infection with *M. luteus, Drs* expression was similarly induced to a high level in both unchallenged flies and flies exposed to *E. muscae* natural infection 48 h prior to *M. luteus* infection, suggesting there was no ongoing suppression of Toll signaling by *E. muscae* (Fig. 3F). Use of flies carrying the *Drs-GFP* reporter revealed similar kinetics of *Drs* expression in 48 h *E. muscae* infected flies and unchallenged flies following infection with *M. luteus* (Fig. 3H). These experiments suggest that natural infection with *E. muscae* fails to activate the Toll pathway rather than suppresses it.

We then compared Toll pathway activity upon septic infection by a needle dipped in spores of *B. bassiana,* or injection of protoplasts of *E. muscae*. As expected, the direct introduction of *B. bassiana* spores triggers a strong *Drs* expression with earlier kinetics compared to natural infection (Fig. 3I). In contrast, injection of *E. muscae* protoplasts did not trigger the Toll pathway more than injury alone as revealed by the low and similar levels of *Drs* expression in both PBS clean injury controls and protoplast-injected flies (Fig. 3J). Expression of another Toll pathway read-out the Bomanin *BomBc3* exhibited similar expression trend to that of *Drs* (Figs. S3F-G). Use of flies carrying the *Drs-GFP* reporter after systemic infection with spores of *B. bassiana* and protoplasts of *E. muscae* further confirmed these observations made by qRT-PCR (Fig. 3K). We conclude that protoplasts are not detected by Toll pathway sensors and that this may provide a mechanism for *E. muscae* to proliferate in the hemolymph without triggering the immune response.

Collectively, our study shows that natural infection with *B. bassiana*, *M. anisopliae* and *M. rileyi* triggers a strong induction of the Toll pathway, consistent with their pathogenicity. Despite its pathogenicity, natural infection with *E. muscae* triggers only a low Toll pathway activity indicating that this fungus is not recognized by the immune system.

279 ***Entomophthora muscae* hides from the host immune response using a vegetative**
280 **development strategy**

281 To explore the strategies employed by *E. muscae* to hide from Toll sensing, we
282 investigated the dynamics of *E. muscae* development inside flies. We first inspected the
283 steps leading to the protoplast-hypha transition *in vitro* by analyzing protoplast
284 differentiation in Grace's insect media. We observed that *E. muscae* protoplasts change
285 from a round to an irregular shape (Fig. 4A). The protoplasts grow and elongate towards
286 both ends and other directions along the sites of vesicle of protoplast. Calcofluor White
287 M2R staining showed the absence of cell walls of these protoplasts before their
288 transformation to hyphae after more than two-weeks culture in the Grace's Insect
289 Medium. We observed the presence of vesicles in both protoplasts and hyphae during
290 the development process in Grace's insect media (red arrow in Figure 4). Vesicles push
291 the membrane outwards, eventually leading to the pinch of the fungal cell to form
292 "subprotoplasts". Vesicles have been demonstrated to promote infection and stimulate
293 protective immunity, depending on the species and host context (Lai et al., 2023; Reis
294 and Rodrigues, 2025; Rodrigues et al., 2024). In addition, DAPI staining reveals that
295 these protoplasts are multinucleated, and in the process of elongating, nuclei disperse
296 along the extension of the protoplasts (Fig. S4). Next, we analyzed protoplast
297 differentiation in flies. Morphology observation of flies showed that the entire
298 infectious process of *E. muscae* could be divided into five stages, namely, early
299 infection stage, fungal spores contact and subsequently penetrate the host cuticle (Stage
300 1/S1), intra-hemolymph growth stage, protoplasts proliferate inside the flies exhibiting
301 erect wings (S2), protoplasts transformed to invasive hyphae stage, flies affixing
302 themselves with their proboscides just prior to death (S3), hyphal growth stage, dead
303 flies with a swollen and white abdomen with full of hyphae in the hemocoel (S4),
304 hyphae extrude and produce spores from the cadavers (S5) (Fig. 4B). Staining fungal
305 cell by dissecting flies at the above stages S1-S5 with Calcofluor White M2R, which
306 marks fungal chitin in the cell wall, reveals that protoplasts undergo differentiation to
307 hyphae only prior to death in the later stages, with no cell wall at S1 and S2, much
308 thinner cell walls at S3 compared to invasive hyphae at S4 and hyphae sporulating on
309 the cadavers at S5 (Fig. 4C). Microscopic observation showed that the development of

310 *E. muscae* protoplasts also underwent the same morphological steps in host hemocoel
311 as observed *in vitro* (Fig. 4A to Fig. 4C). Although protoplasts undergo the same
312 differentiation process in infected flies, the transition from protoplasts to hyphae takes
313 place 4 to 7 days after fly infection, compared to two weeks in the Grace's Insect
314 Medium. Thus, the formation of invasive hyphae is a process that take place very late
315 in the infection process, just before fly death. The observation that injection of *E.*
316 *muscae* protoplasts are not recognized by the immune system, and that *E. muscae*
317 persists in the first stage of infection as protoplasts, suggests that this fungus hides from
318 the immune system by using a cell wall-less structure.
319

320 **The Persephone branch of the Toll-PO serine protease cascade is more critical**
321 **than the GNBP3 -modSP branch to activate the Toll pathway**

322 The Toll pathway is activated upon the maturation of the Toll ligand Spz by a
323 complex cascade of serine proteases called the Toll-PO serine protease (SP) cascade,
324 which also regulates the maturation of PPOs (Westlake et al., 2024). Lysine-type
325 peptidoglycans from Gram-positive bacteria and β-glucans from fungi are detected by
326 the pattern recognition receptors (PRRs) PGRP-SA (with its adaptor GNBP1) and
327 GNBP3, respectively (Gottar et al., 2006; Michel et al., 2001) This triggers the
328 sequential activation of SPs ModSP, Grass, and Psh/Hayan (Buchon et al., 2009; Dudzic
329 et al., 2019; El Chamy et al., 2008; Kambris et al., 2006). Psh and Hayan mediate the
330 activation of SPE, which cleaves Spz, which then dimerizes and binds to the Toll
331 receptor inducing an intracellular cascade leading to the production of Toll-regulated
332 effectors such as antimicrobial peptides (Jang et al., 2006; Weber et al., 2003). Psh (and
333 likely Hayan) can also be independently cleaved by microbial proteases (El Chamy et
334 al., 2008; Gottar et al., 2006; Issa et al., 2018). Hayan and Psh also regulate downstream
335 SPs that activate PPO1 and PPO2, initiating the melanization response leading to
336 cuticular blackening and microbicidal activities (Fig. 5A) (Dudzic et al., 2019; Nam et
337 al., 2012; Shan et al., 2023; Westlake et al., 2024). Having shown the critical role of the
338 Toll pathway upon natural infection with entomopathogenic fungi, we investigated the
339 mechanisms that activate Toll focusing on *B. bassiana*, *M. anisopliae, M. rileyi* and *E.*
340 *muscae*. In these experiments, we used flies carrying the *GNBP3*^{hades} null mutation over

341 a deficiency *Df(ED4421),* as we noticed that *GNBP3*^{hades} homozygous flies display a
342 marked susceptibility to fungal infection that was not observed in transheterozygote
343 *GNBP3*^{hades}*/Df(ED4421)* flies, pointing to a background effect (Figs. S5A and 5B). The
344 marked susceptibility of the *psh*^{SK1} analysis showed that Psh contributes to resistance
345 to *B. bassiana*, *M. anisopliae, M. rileyi* and *E. muscae* (Figs. 5B-E). In contrast, the role
346 of the glucan binding sensor GNBP3 was modest as revealed by the almost wild-type
347 resistance of *GNBP3*^{hades}*/Df(ED4421)* flies to *B. bassiana*, *M. anisopliae, M. rileyi* and
348 *E. muscae* (Figs. 5B-E, Table S4). Similar results were obtained when using another
349 recently generated *GNPB3*$^{\Delta}$ deficient mutant (Lu et al., 2024) (Figs. S5A and S5B). As
350 ModSP integrates signals from GNBP3 as a PRR of the Toll-PO SP cascade (Buchon
351 et al., 2009), we expected that *modSP*^{1} flies would exhibit the same resistance as
352 *GNBP3*^{hades}*/Df (ED4421)* flies to fungal infection. We indeed observed that *modSP*^{1}
353 flies exhibited the same ability as *GNBP3/Df (ED4421)* flies to survive *B. bassiana*, *M.*
354 *anisopliae* and *M. rileyi (*Fig 5B-D). Strikingly, *modSP*^{1} flies but not
355 *GNBP3/Df(ED4421)* displayed a marked susceptibility to *E. muscae* similar to *spz*^{rm7}
356 flies (Fig 5E). As expected, *psh*^{1}*;;modSP*^{1} double mutants that block both modes of
357 sensing of Toll and *Hayan-psh*^{Def} double mutants displayed susceptibility similar to
358 *spz*^{rm7} flies. To further characterize the role of the Toll sensor, we next monitored Toll
359 pathway activation upon natural infection with *M. anisopliae*. We restricted our analysis
360 to this fungal species as *M. anisopliae* strongly activates the Toll pathway. The
361 expression pattern of *Drs* and *BomBc3* in the mutants confirms the main role of Psh in
362 activation of the Toll pathway upon natural infection (Figs. 5F-G). Both *Drs* and
363 *BomBc3* expression were not induced in *psh*^{SK1} flies, *Hayan-psh*^{Def} double mutant flies,
364 or *psh*^{1}*;;modSP*^{1} double mutant flies, being comparable to *spz*^{rm7} flies, consistent with
365 their high susceptibilities to fungal infection. However, the expression of the Toll
366 pathway was not affected in *GNBP3*^{hades} homozygous flies as revealed by the wild-type
367 expression of *Drs* and *BomBc3*.

368 We conclude that Psh is a highly important sensor in activating the Toll pathway to
369 mediate the resistance against these fungi, while GNBP3 plays only a minor role.
370 Surprisingly, we note that ModSP plays a specific role in resisting infection with *E.*
371 *muscae*, suggesting another role of this apical serine protease beyond integrating

372 GNBP3 signals.

373

374 **The Toll pathway restricts fungal growth**

375 Having characterized the importance of the Toll pathway and the underlying
376 mechanism leading to its activation, we next explored how the Toll pathway effectively
377 combats fungal infection. Protection by the immune system can be mediated via
378 resistance mechanisms that prevent pathogen growth or via tolerance mechanisms that
379 protect the host without directly inhibiting the pathogen (Pradeu et al., 2024; Soares et
380 al., 2017). We infected flies by natural infection and quantified fungal proliferation after
381 infection. qPCR levels of *B. bassiana 18S* gDNA reveal a much high fungal load at 3-
382 and 4-days post natural infection in spz^{rm7} flies compared to wild-type flies (Fig. 6A).
383 Higher fungal loads with earlier growth kinetics were also found in spz^{rm7} flies
384 compared to wild-type flies when infected with *M. anisopliae* and *E. muscae* (Figs. 6B-
385 C). To confirm and extend these results, we used a *M. anisopliae* tagged GFP strain and
386 monitored the expression of the Green Fluorescent Protein (GFP) upon septic infection
387 in both wild-type and *spz* mutant flies. We observed a much higher proportion of flies
388 with strong GFP signals in spz^{rm7} flies compared to wild-type (Fig. 6D). While *M.*
389 *anisopliae* disseminated throughout the body in spz^{rm7} mutant flies, the fungus was
390 restricted to the thorax in wild-type flies at 2- and 3- days post infection (Fig. 6E). In
391 keeping with this faster dissemination, the fungi broke through cuticle and extrude from
392 the cadavers of spz^{rm7} mutant flies 2 to 4-day before that of wild-type flies. In both wild-
393 type and spz^{rm7} flies, fungal growth eventually occurs in the cadavers across all three
394 tagmata, including the wings and legs (Fig. S6). We conclude that Toll act as a resistance
395 mechanism limiting the growth of these three entomopathogenic fungi.

396

397 **Multiple host defense peptides contribute to Toll antifungal activity**

398 In the last years, several host new defense peptides controlling fungal infection have
399 been identified in *Drosophila* (Hanson et al., 2025). In addition to Drs and Mtk that
400 display antifungal activity *in vitro* (Feldman et al., 2019; Moghaddam et al., 2017),
401 genetic studies have revealed that deficiencies in *Baramicin A*, *Bomanins* (12 genes)
402 and *Daisho* (2 genes) cause susceptibility to specific fungi (Clemmons et al., 2015;

Cohen et al., 2020; Hanson et al., 2021). The role of these immune peptides has never been analyzed collectively for their role in host defense to fungi. This prompted us to explore the nature of downstream Toll effectors using isogenic mutant lines against entomopathogenic fungi upon natural infection. In this analysis we used single null mutants in *Drosomycin* (Drs^{R1}), *Metchnikowin* (Mtk^{R1}), *Baramicin A* ($BaraA^{SW1}$), *Daisho1/2* ($^{\Delta}Dso$, a short deletion removing both Daisho 1 and 2) and $Bom^{\Delta 55C}$ that removes ten of the twelve *Bomanins* (Clemmons et al., 2015; Cohen et al., 2020; Hanson et al., 2021, 2019). We also used previously generated compound mutants including Mtk^{R1}, Drs^{R1} double mutants, $^{\Delta}$AMP10 (a fly line deleted for 10 AMPs including *Mtk*, *AttA/B/C/D*, *DptA/B*, *Drc*, *Def*) and $^{\Delta}$AMP14 (a fly line deleted for 14AMPs similar to $^{\Delta}$AMP10 with an additional deletion of the four *Cecropin* genes *CecA1/A2/B/C*) flies (Carboni et al., 2022; Hanson et al., 2019). In the framework of this study, we further generated four additional compound mutants to see possible additivity or synergistic action of these host defense peptides including i) $BaraA^{SW1}$, $^{\Delta}Dso$; ii) Mtk^{R1}, $BaraA^{SW1}$; Drs^{R1}; iii) Mtk^{R1}, $BaraA^{SW1}$, $^{\Delta}Dso$; Drs^{R1}) and iv) Mtk^{R1}, $Bom^{\Delta 55C}$; Drs^{R1}.

Upon natural infection by fungi, the $Bom^{\Delta 55C}$, $^{\Delta}Dso$ deletions caused marked susceptibility to all four entomopathogenic fungi while single mutations in *Mtk* and *Drs* had no effect against any fungus. Alone, $BaraA^{SW1}$ caused a susceptibility to only two of the four fungi. This reveals the critical role of Bomanin and Daisho1/2 to resist fungal infection (Fig. 7A and Fig. S7). We found that flies lacking both *Baramicin* and *Daisho1,2* were markedly more susceptible to infection with *B. bassiana, M. rileyi,* and *E. muscae*, compared to $^{\Delta}Dso$ single mutant flies, while the difference for *M. anisopliae* was consistent in direction, but relatively minor (Tables S5 and S8). We also observed that Mtk^{R1}, Drs^{R1} but not Mtk^{R1} or Drs^{R1} single mutants display increased susceptibility to *M. anisopliae*, but not *B. bassiana*, *M. rileyi* and *E. muscae,* revealing an additive effect against *M. anisopliae* specifically. Strikingly, Mtk^{R1}, $Bom^{\Delta 55C}$; Drs^{R1} showed greater susceptibility to infection compared to $Bom^{\Delta 55C}$ flies for *B. bassiana, M. anisopliae,* and *M. rileyi,* but not *E. muscae*. The susceptibility of Mtk^{R1}, $Bom^{\Delta 55C}$; Drs^{R1} flies was slightly but consistently less marked than spz^{rm7} mutant flies across all fungi. Finally, we observed that *ΔAMP14* flies display greater susceptibility compared

434 to *⊿AMP10* flies against each fungus, pointing to a role of Cecropin in host defense
435 against fungi, consistent with *in vitro* observation (Ekengren and Hultmark, 1999).
436 Taken together, our study reveals that host defense peptides regulated by the Toll
437 pathways, notably Bomanins, Daisho1/2, BaraA, Mtk and Drs largely explain the
438 contribution of Toll to resist fungus natural infections. The strength of effect was
439 broadly consistent across fungal species, with virulent species revealing a greater
440 resolution of differential susceptibilities. Generally, we did not find evidence for a
441 specific importance of any fungus-by-gene interactions among these effectors,
442 suggesting their contributions to survival are based on their collective action in
443 antifungal defense, with some being more important than others.
444
445 **Both PPO1 and PPO2 additively contribute to host defense against fungi**
446 Having described the contribution of Toll effectors, we next analyzed how
447 melanization contributes to host defense against these entomopathogenic fungi.
448 Previous studies have shown that PPO1 and PPO2 redundantly contribute to both
449 cuticular and hemolymphatic melanization (Binggeli et al., 2014; Dudzic et al., 2019).
450 Genetic approaches have allowed us to distinguish distinct activities associated with
451 PPO1 and PPO2: cuticular melanization at the injury site is dependent on PPO1
452 activated through Hayan, while an uncharacterized microbicidal activity against
453 *Staphylococcus aureus* relies on Sp7, but not Hayan, with a major role for PPO1 and a
454 lesser but important role for PPO2 (Dudzic et al., 2019); we will note, however, that
455 there is some redundancy *in vitro* regarding the capability of these SPs to cleave PPO1
456 and PPO2 (Shan et al., 2023). Surprisingly, compared to these roles against *S. aureus,*
457 we confirmed a consistent but opposite trend in the importance of *PPO1* and *PPO2* in
458 defense against natural infection by each fungus (Fig. 7B and Fig. S8). *PPO2* mutants
459 were more susceptible to all fungi compare to PPO1, although *PPO1, PPO2* double
460 mutants were consistently more susceptible than flies deleted for *PPO2* alone (Tables
461 S6 and S8). We next tested deletions in *Hayan* (*Hayan*^{SK6}) and *Sp7* (*Sp7*^{SK6}). Agreeing
462 with a primary role of Sp7 in PPO2-mediated defense, *Sp7*^{SK6} flies were as susceptible
463 to natural infection by *B. bassiana* and *M. anisopliae* as *PPO2* mutants. On the other
464 hand, *Hayan* mutation caused no susceptibility to *B. bassiana,* but a similar

465 susceptibility to *Sp7* and *PPO2* mutants to *M. anisopliae.* No single mutation caused a
466 significant mortality against *M. rileyi.* Strikingly, *Hayan* mutation, but not *Sp7*, had a
467 comparable susceptibility to *PPO2* mutants to *E. muscae.* In all cases, spz^{rm7} was the
468 most susceptible genotype.

469 We also monitored fungal load of *B. bassiana* and *M. anisopliae* in these genotypes
470 at key time points after infection. qPCR of *B. bassiana 18S* and *M. anisopliae Rpl32*
471 revealed trends broadly consistent with survival curves, with higher fungal loads
472 broadly correlating to survival (Figs. 8A-B). We also infected wild-type and
473 melanization deficient flies by pricking with *M. anisopliae* GFP spores in the thorax. In
474 these experiments bypassing the cuticle, we again observed faster growth of *M.*
475 *anisopliae GFP* in $PPO1^{\Delta}$, $PPO2^{\Delta}$ flies revealed by stronger GFP signals and higher
476 dissemination level within the body at both 2- and 3-day post-infection compared to
477 wild-type flies (Fig. 8C). Consistent with the survival analysis, we observed slightly
478 faster growth *M. anisopliae-GFP* in *PPO2* single mutants compared to *PPO1* single
479 mutants, with a slightly earlier and stronger GFP signal also seen for *Hayan* and *Sp7*
480 deficient flies both at 48 h and 72 h after pricking compared to wild-type and *PPO1*
481 mutants (Fig. 8C).

482 Collectively, our study reveals a stronger role of PPO2 compared to PPO1 in defense
483 against fungi. Additionally, it reveals different requirements for Sp7 and Hayan in
484 defense against these fungal species, somewhat agreeing with previous observations for
485 the role of these serine proteases in activating PPO1 or PPO2 in defense against *S.*
486 *aureus,* although there is some additional complexity to the antifungal response. There
487 was a strong correlation between susceptibility and fungal growth in the tested mutants,
488 indicating that melanization contributes to host survival by limiting fungal
489 dissemination and growth.

490

491 **Higher Toll pathway activity in $PPO1^{\Delta}$, $PPO2^{\Delta}$ mutant**

492 Finally, we explored whether the immune susceptibility of melanization defective
493 flies might result from improper Toll activity in the absence of melanization, we
494 monitored the activation of the Toll pathway in *PPO1*, *PPO2* single and double mutant
495 flies as well as *Sp7* and *Hayan* flies. Single mutations in *PPO1*, *PPO2*, *Sp7* and *Hayan*

did not affect the inducibility of *Drosomycin* upon natural infection with *M. anisopliae* and *B. bassiana* (Figs. S9A-B). In agreement with previous studies (Binggeli et al., 2014; Ryckebusch et al., 2025), we found a trend of higher Toll pathway activation in *PPO1*$^{\Delta}$, *PPO2*$^{\Delta}$ double mutant flies compared to wild-type flies upon natural infection with these two fungal species, although *PPO* single mutants showed no increased Toll activity. A higher and earlier Toll pathway activation was also observed upon direct introduce of *M. anisopliae* spores in the body cavity at the time points of 24 h and 48 h, but not 72 h (Fig. S9C). Interestingly, we also observed a higher level of *Drs* expression in *PPO1*$^{\Delta}$, *PPO2*$^{\Delta}$ flies compared to wild-type flies upon injury with a clean needle. Moreover, unchallenged *PPO1*$^{\Delta}$, *PPO2*$^{\Delta}$ flies tend to have higher basal expression of *Drs* compare to their wild-type counterpart across each time point (Fig. S9C).

We conclude that higher Toll signaling in *PPO1*$^{\Delta}$, *PPO2*$^{\Delta}$ is not strictly linked to higher fungal load, but may relate to a negative feedback loop between the Toll and the melanization cascade. This negative feedback loop has been proposed previously using live and heat-killed microbe injections (Binggeli et al., 2014; Ryckebusch et al., 2025). Here we show this increased Toll activity is true even for unchallenged and clean injury treatments, suggesting a role for PPOs in regulating Toll activation even in the absence of infection.

Discussion

Host–fungal pathogen interactions are complex and serve as potent drivers of evolutionary diversification (Brown, 2023; Gladieux et al., 2014; Murante and Hogan, 2024; Shang et al., 2016). Fungal pathogens span a broad ecological spectrum -from generalists like *B. bassiana* and *M. anisopliae* with wide host ranges, to specialists such as *M. rileyi*, *E. muscae*, and *O. sinensis*, to opportunistic fungi like *C. albicans* and *A. fumigatus*. Despite this diversity, our understanding of how fungal pathogens with distinct lifestyles interact with host immunity remains incomplete (Lu et al., 2024; Murante and Hogan, 2024; Qu and Wang, 2018; Wang and Wang, 2017).

To address this gap, we used *Drosophila melanogaster* lines deficient in specific immune pathways and effectors (Hanson et al., 2023, 2019; Ryckebusch et al., 2025), systematically investigating host defense against five fungal species. Consistent with

earlier work (Lemaitre et al., 1996; Ryckebusch et al., 2025; Westlake et al., 2024), the Toll pathway emerged as the most critical immune module for defense against all tested fungi. Generalist pathogens like *B. bassiana* and *M. anisopliae*, and to a lesser extent the specialist *M. rileyi*, strongly induced the Toll pathway reporter gene *Drs* upon natural infection. In contrast, *E. muscae* triggered only weak activation, and *A. fumigatus* did not induce *Drs* expression at all. Nevertheless, Toll signaling remained essential for survival even against weak inducers, suggesting that basal or low-level Toll activity is sufficient to confer protection.

Our findings further show that Toll pathway-mediated immunity is important not only after natural infection, which involves cuticle penetration, but also after systemic infections when fungal spores are introduced directly into the hemolymph. This emphasizes the role of the Toll pathway in limiting fungal growth systemically. Recent studies using deletions of immune effectors downstream of the Toll and Imd pathways have demonstrated synergistic, additive, and pathogen-specific roles in survival (Hanson et al., 2025, 2019). We show here that Bomanins and Daisho peptides are essential for resisting infection by generalist and specialist entomopathogenic fungi. These observations align with previous studies showing the broad antifungal activity of Bomanins against *Fusarium spp.*, *B. bassiana*, *M. anisopliae*, and yeast species (Clemmons et al., 2015; Hanson et al., 2019), and Daisho peptides active against *Fusarium* species and some *Aspergillus* strains (Cohen et al., 2020). In addition, Baramicin A peptides are important for defense against virulent *Beauveria* and *Metarhizium* species (Hanson et al., 2021; Huang et al., 2023), while an individual importance for Drosomycin and Metchnikowin was not observed for any fungus tested (Hanson et al., 2021, 2019). However, the Baramicin, Drosomycin, and Metchnikowin peptides each contribute to defense independently from other Toll effectors, evidenced by a increased mortality of *BaraA, Dso* and *Drs, Mtk, Bom* combinatory mutants against most fungi. Our results may help make sense of previous studies showing striking single-mutant susceptibilities (Cohen et al., 2020; Hanson et al., 2021), as the importance of these genes was revealed in a virulence-dependent, or host susceptibility-dependent, manner – virulence and susceptibility broadly measuring opposite sides of the same coin. Thus, unlike the specificity observed for antibacterial peptides (Hanson

et al., 2023, 2019; Unckless et al., 2016), the antifungal peptides we tested appear to act in a more general fashion, suggesting that they target broadly conserved fungal features. The similar susceptibility profiles of *BaraA*^{SW1}, *Mtk*^{R1}, $^{\Delta}$*Dso; Drs*^{R1} mutants to *Bom*$^{\Delta 55C}$ underscores the critical role of these humoral Toll-mediated effectors in antifungal immunity, with additional mutations (e.g. *Mtk*^{R1}, *Bom*$^{\Delta 55C}$*; Drs*^{R1} flies) increasingly approaching *spz*^{rm7} levels of susceptibility. It would be interesting to achieve the full Toll effector combinatory mutant line (*BaraA*^{SW1}, *Mtk*^{R1}, *Bom*$^{\Delta 55C}$, $^{\Delta}$*Dso; Drs*^{R1}) to learn if there is any resistance mediated by *spz* beyond the contributions of these five effector families.

As our *Bom*$^{\Delta 55C}$ and *⊿Dso* deletions removed large gene clusters (10 of 12 Bomanins and both Daisho genes), we could not assess individual gene contributions. However, recent work has identified roles for specific Bomanins such as BomT1 and BomT2 in resisting *Enterococcus faecalis*, *M. robertsii*, and *A. fumigatus* ribotoxins (Lou et al., 2025). Identifying the Bomanins that mediate defense against the fungi tested here will be an important next step. In addition, it would be interesting to confirm the precise mechanism through which Cecropins improve survival against entomopathogenic fungi, as while these peptides can display antifungal activity *in vitro*, AMPs also regulate the host microbiota in *Drosophila* (Marra et al., 2021). The protective effect of Cecropins could therefore rely either on a direct antifungal action, or an indirect role in preventing dysbiosis, perhaps also modulating the cuticle microbiota that itself protects against topical fungal infections (Hong et al., 2022).

Unexpectedly, we did not observe a major contribution of the glucan sensor GNBP3 in activating Toll in response to *M. anisopliae*. A recent study showed that GNBP-like3 (GL3) acts as a bait for the fungal effector Tge1, which can inhibit GNBP3 and so suppress Toll immune activation (Lu et al., 2024); GL3 itself does not propagate Toll signaling. However, our results using *GNBP3, GNBP3/Df(ED4421)* indicate a minor role only for this GNBP3 arm of Toll signaling in survival upon *B. bassiana* and *M. anisopliae* natural infection (Fig. S5). Instead, our data support a predominant role for the Persephone (Psh) branch of Toll activation, suggesting that entomopathogenic fungi are primarily recognized via the proteases they secrete (Gottar et al., 2006). These include serine proteases and chitinases involved in cuticle degradation (Qu and Wang,

2018), to which Psh may be specifically adapted.

Melanization also contributed to host defense, albeit to a lesser extent than Toll signaling, consistent with earlier findings (Binggeli et al., 2014; Ryckebusch et al., 2025). Its reduced impact upon septic infection suggests a key role at the initial cuticular breach, where melanin and ROS deposition may restrict fungal entry and dissemination. This is consistent with observations in *Galleria mellonella* and *Anopheles gambiae*, where melanin accumulates at fungal entry sites (Vertyporokh et al., 2020; Yassine et al., 2012).

We show that both PPO1 and PPO2 contribute to fungal resistance. Interestingly, across fungal pathogens we found PPO2 plays a more prominent role in host defense compared to PPO1, even after septic injury with *M. anisopliae*. Previous studies have described a major role for PPO1 in wound site melanization through the action of Hayan, but also PPO1 in resistance to *S. aureus* in a Hayan-independent manner, with a more minor role for PPO2 (Binggeli et al., 2014; Dudzic et al., 2019). However, here using entomopathogenic fungal infections, we found the opposite. Unlike the case of *S. aureus*, distinct roles for *Hayan* and *Sp7* in this PPO2-mediated resistance are less clear, perhaps reflecting an importance of Sp7 in the hemolymph, and of Hayan as the PPO-converting SP at the injury site suggested by its essentiality for wound blackening (Dudzic et al., 2019); however, wound site blackening requires Hayan acting through PPO1. We also observed higher Toll pathway activation in *PPO1, PPO2* double mutant flies compared to wild-type flies upon fungal natural infection, agreeing with previous studies (Binggeli et al., 2014; Ryckebusch et al., 2025). Here we additionally show this higher Toll activation upon clean injury and even in unchallenged flies. This suggests that byproducts of POs somehow regulate Toll activation, which include terminal reactive oxygen species, but also various intermediates involving the conversion of tyrosine to L-DOPA and derivatives such as dopaquinone or the production of melanin from 5,6-dihydroxyindole (DHI) (Westlake et al., 2024). Conversely, Dopa decarboxylase converts L-DOPA to dopamine, and so the deficiency of PO activity converting L-DOPA to dopaquinone could result in the inverse accumulation of dopamine, likely having pleiotropic effects. These observations provide a mechanistic basis for future exploration. Here, the higher Toll activity in *PPO1, PPO2* double

mutant flies suggests there is effectively negative feedback exerted by the melanization pathway on the Toll pathway. It would also be interesting to know if this role of melanization in Toll regulation is related to the role of both modules in the wound healing response (Capilla et al., 2017; Carvalho et al., 2014).

The Imd pathway and cellular immunity had minimal roles in resistance to the four entomopathogenic fungi tested, except for a contribution of Imd during *A. fumigatus* septic infection. Interestingly, volatile organic compounds from *A. fumigatus* have been shown to be toxic to Imd-deficient flies (Almaliki et al., 2023), and a previous study showed that *A. fumigatus* virulence acted through either proliferation or secretion of toxins in a Bomanin and melanization-dependent manner (Xu et al., 2023), suggesting *A. fumigatus* deploys multiple pathogen strategies that interact with different arms of host immunity. While the cellular response is important against yeast like *C. glabrata* (Quintin et al., 2013), filamentous fungi may evade phagocytosis due to their morphology -hyphae being more difficult to phagocytose because of their length.

A key aim of our study was to compare *Drosophila* immune responses to fungi with distinct ecological strategies. Despite lifestyle differences, we found a largely conserved requirement for Toll signaling, antifungal peptides, and melanization across all species tested. However, notable differences emerged. The two generalist entomopathogenic species strongly activate the Toll pathway but can overcome Toll effectors to infect and kill flies. Studies have shown that these species express many virulence factors that likely confers them protection against the host immune system (Gao et al., 2011; Hu et al., 2014; Wang and Wang, 2017; Yuan et al., 2020). In contrast, *A. fumigatus* is weakly pathogenic upon natural infection and accordingly does not activate the Toll pathway. This opportunistic fungus does not have the ability to effectively cross the cuticle of *Drosophila*, reflecting an opportunistic lifestyle. In contrast the specialist noctuid-virulent fungus *M. rileyi* was moderately pathogenic to flies and only triggered the Toll pathway at a late time point. This may reflect the proliferation of this species within the host, rather than toxin-mediated pathogenesis as seen in *B. bassiana* and *M. anisopliae* during fly colonization (Boucias et al., 2016; Schrank and Vainstein, 2010; Wang and Wang, 2017; Wang et al., 2021). Strikingly, we observed that *E. muscae* was greatly pathogenic to flies but did not trigger a strong Toll

pathway response. Nevertheless, the Toll and melanization modules do contribute to host defense to *E. muscae* indicating that this species is also sensitive to immune effectors. Our study finds that *E. muscae* has developed a specific colonization strategy to escape the host immune response. After crossing the cuticle barrier and reaching the hemolymph, *E. muscae* grows as multinucleated protoplasts undetected by the immune system. The absence of cell wall in protoplasts results in little glucan release into the hemolymph, which might prevent recognition. This strategy would explain the high pathogenicity of *E. muscae,* allowing growth hidden from the immune system, and only differentiating into thinner cell-walled hyphae only shortly before the death of the host. Similar escape strategies to hide from the host immune response have been described in specialists such as *M. rileyi* and *O. sinensis* (Boucias et al., 2016; Li et al., 2020; Liu et al., 2019). Unlike *E. muscae* protoplasts, *M. rileyi* and *O. sinensis* grow as yeast-like blastospores with a thinner cell wall than their conidia (Boucias et al., 2016; Liu et al., 2019). Thus, two distinct infection strategies emerge among entomopathogenic fungi: (1) Generalists, such as *B. bassiana* and *M. anisopliae*, mount an aggressive infection, are immediately recognized by the immune system, and rely on a broad array of virulence factors to counter host defenses (Gao et al., 2011; Schrank and Vainstein, 2010; Wang et al., 2021); and (2) Specialists, such as *E. muscae*, *M. rileyi*, and *O. sinensis*, adopt stealthier strategies, growing initially in immunoevasive forms before transitioning to lethal hyphal stages. These strategies appear to correlate with the fast and slow timing of host infection: for example, *O. sinensis* persists for months in *Thitarodes* larvae, only initiating pathogenic development later (Liu et al., 2019; Meng et al., 2015; Rao et al., 2019). Similarly, the slow-growing, behavior-manipulating *E. muscae* may rely on immune evasion to enable host manipulation and spore dispersal.

Taken together, our study clarifies the immune strategies employed by *D. melanogaster* to combat fungal infections. We further provide insight on how entomopathogenic fungi circumvent the immune response. Our study complements the recent identification of fungal virulence factors required to disarm the immune system (Lu et al., 2024; Shang et al., 2023; Tang et al., 2025). The interplay between local and systemic immune responses highlights the complexity of antifungal defense mechanisms in *Drosophila*. Understanding the evolutionary pressures that shape

682 immune responses to fungal pathogens could have broader implications for controlling
683 fungal infections in both natural and agricultural settings.
684
685 **Materials and methods**
686 **Fly stocks**
687 The fly stocks iso w^{1118} drosdel wild-type was used as the genetic background for
688 mutant isogenization (Ferreira et al., 2014). For survival experiments, w^{1118} *drosdel*,
689 Oregon R or Canton S flies were used as wild-type controls. To determine the
690 contribution of the four main immune modules to resist different fungal species, the
691 *Relish* (Rel^{E20}), *spätzle* (spz^{rm7}), *PPO1* and *PPO2* double mutant ($PPO1^{\Delta}$, $PPO2^{\Delta}$),
692 $NimC^{1}$ and *eater* double mutant ($Nim\ C1^{1}$; $Eater^{1}$) (Binggeli et al., 2014; Dudzic et al.,
693 2019; Hedengren et al., 1999; Lemaitre et al., 1996; Melcarne et al., 2019) were used.
694 The fly line devoid of all four immune modules: Imd, Toll, Phagocytosis and
695 Melanization [genotype: *Def(Hayan-psh)*; *NimC1; Eater*, $Relish^{E20}$] (Ryckebusch et al.,
696 2025) is used to investigate whether immune modules function independently or
697 synergistically to combat different fungi.
698 To compare the importance of Toll sensing pathway, we used flies lacking Hayan
699 ($Hayan^{SK6}$), Psh (psh^{SK1}), both Hayan and Psh ($Hayan\text{-}psh^{def}$) (Dudzic et al., 2019),
700 Gram-negative bacteria binding protein 3 ($GNBP3^{hades}$) (Gottar et al., 2006), ModSP
701 ($modSP^{1}$), both Psh and ModSP ($psh^{1};;modSP^{1}$) (Buchon et al., 2009).
702 To determine the role of host defense peptides to combat fungal infection, we used
703 flies deleting ten of the twelve Bomanins ($Bom^{\Delta 55C}$) (Clemmons et al., 2015) and flies
704 lacking Metchnikowin (Mtk^{R1}), Drosomycin (Drs^{R1}) (Hanson et al., 2019), Baramicin
705 ($BaraA^{\Delta}$) (Hanson et al., 2021), Daisho 1, 2 ($^{\Delta}Dso$) (Cohen et al., 2020), as well as
706 compound mutants Mtk^{R1};Drs^{R1}, $\Delta AMP10$ and $\Delta AMP14$ (Carboni et al., 2022; Hanson
707 et al., 2019). In this study, we generated four new compounds mutants lack host defense
708 peptides in the Drosdel background, ($BaraA^{SW1}$, ΔDso); (Mtk^{R}, $BaraA^{SW11}$; Drs^{R1});
709 (Mtk^{R}, $BaraA^{SW1}$, ΔDso^{1}; Drs^{R1}) and (Mtk^{R1}, $Bom^{\Delta 55C}$; Drs^{R1}). The wild-type and
710 mutant flies used in this study are listed in Table S1.
711
712

713 **Microbial cultures**

714 The wild type strains of *B. bassiana* 802, *M. anisopliae* ARSEF 2575, *M. rileyi*
715 PHP1705 and the genetic strains *M. anisopliae* tagged GFP were cultured on malt agar
716 (1g Bacteriological Peptone, 20g Glucose, 20 g Malt Extract, 15 g Agar, with the
717 addition of water to the total volume of 1 liter) at 29°C for two weeks for harvesting
718 conidial spores. The wild type strain *A. fumigatus* was cultured on malt agar at 37°C for
719 one week for harvesting spores. Fungal materials were then strained through three
720 layers of precision wipes with sterile water to collect spores, which were resuspended
721 with 0.05% Tween 80 before being used for infection. The *E. muscae* ARSEF 454 was
722 cultured in Grace's Insect Medium supplemented with 10% fetal bovine serum at 21°C.
723 A liquid of 1 ml growing cultures after three weeks culture was transferred to a new
724 cell culture flask with the addition of 10 ml media to maintain the fungal strains *in vitro*.
725 The Gram-positive bacteria *Micrococcus luteus* were cultured on Luria Broth at 37°C
726 and the optical density of the pellet (O.D.) at 600 nm 200 were used for infection.

727

728 **Survival experiments**

729 Survival experiments were conducted by both topical infection (natural infection)
730 and systemic infection (septic infection), with twenty 2- to 4-day-old adults per vial
731 with two to three replicate experiments. All experiments were conducted with male flies
732 unless otherwise indicated. Topical infection assays were performed by immersing flies
733 in spore suspensions for 30 s. The following concentrations (in spores/ml) of spore
734 suspensions were used: *A. fumigatus, B. bassiana* and *M. rileyi*: 1×10^9; *M. anisopliae*:
735 5×10^8. For *E. muscae* natural infection, about twenty-five 1- to 2-day-old adult male
736 flies were infected by spore shower from twenty freshly emerged cadavers that were
737 previously injected with protoplasts for 24 h. The average spores ejected from each
738 female or male fly for 24 h were evaluated as described in (Edwards and De Fine Licht,
739 2024). Briefly, the head of the cadaver was insert into Vaseline inside the lid of the 2
740 ml tube containing 1ml 1% Triton-X and 0.2% maleic acid solution for a period 24 h to
741 collect ejected of spores. Then, spores in solution were counted on a hemocytometer
742 under a microscope. Systemic infections were performed by pricking 2- to 4- day-old
743 adult males in the thorax with a 100 µm-thick insect pin dipped into spore suspensions.

744 The following concentrations (in spores/ml) of spore suspensions were used: *B.*
745 *bassiana, M. anisopliae* and *M. rileyi*: 1×10^8, *A. fumigatus*: 1×10^9. Infected flies were
746 flipped at the end of the first day and maintained at 29°C and flipped every two days
747 later. Systemic infection with *E. muscae* was performed by injecting 23 nl of protoplast
748 suspension per fly with a concentration of 2×10^6 protoplasts/ml in PBS. The mortality
749 was recorded daily. At least three independent experiments for survival to infection
750 were performed with 20 flies per vial on standard fly medium.
751
752 **Gene expression levels by RT-qPCR**
753 To investigate the immune responses to fungal infections, we performed the
754 quantitative reverse transcription PCR (qRT-PCR) analysis of Drs and BomBc3 used as
755 read-outs of Toll pathway activity. About 10 adult flies were collected at indicated time
756 points and homogenized for RNA extraction using TRIzol reagent. The total RNA was
757 resuspended in RNase-free water and 0.5 mg of total RNA in 10 ml reactions was
758 reverse transcribed using PrimeScript RT (TAKARA) with random hexamer and oligo
759 dT primers. Quantitative PCR was performed on a LightCycler 480 (Roche) in 96-well
760 plates using PowerUp SYBR Green Master Mix. Primers were listed in Table S7. The
761 expression of *Drs* was also investigated by observing GFP intensity of *Drs-GFP* flies
762 after fungal infection (Ferrandon, 1998). Infected flies were anesthetized with CO_2 and
763 observed for fluorescence with a Leica Application SuiteX and LEICA DFC 7000T
764 camera.
765
766 **Quantitation of fungal loads for kinetic growth**
767 Fungal load in infected flies was measured either by qPCR or by fluorescence
768 intensity of *M. anisopliae t*agged GFP. Adult male flies infect with *B. bassiana* and *M.*
769 *anisopliae* were incubated at 29°C and *E. muscae* at 21°C. Groups of 10 flies were
770 sampled at indicated time points and frozen in liquid nitrogen. The total DNA of each
771 sample was extracted with DNeasy Plant Mini Kit (Qiagen). Fungal loads of *B.*
772 *bassiana* and *E. muscae* was quantified by fungal ribosomal protein 18S rRNA relative
773 to the *Drosophila* ribosomal protein Rpl32 (Rp49), while fungal load of *M. anisopliae*
774 was quantified by fungal ribosomal protein Rpl32 relative to *Drosophila* protein Actin.

775 Primers were listed in Table S7.

776 *M. anisopliae* tagged GFP was also used to investigate the growth of fungi inside the
777 flies after pricking. The infected flies were anesthesized with CO_2 and observed for
778 fluorescence with a Leica Application SuiteX and LEICA DFC 7000T camera.

779

780 **Statistical analysis**

781 Statistical analyses were performed using GraphPad Prism 10 software. Survival
782 experiments were repeated at least three times independently with 20 flies per treatment.
783 Statistical significance of survival data was calculated with a log-rank test comparing
784 each genotype to w^{1118} flies. Quantitative PCR data and fungal load data were compared
785 by One-way ANOVA following Tukey's multiple comparisons test. The full statistic
786 models and outputs of Figures are listed in Table S8. P values of < 0.05 = *, < 0.01 =
787 **, < 0.001 = ***, and < 0.0001 = **** were considered significant. ns indicates non-
788 significant, P>0.05. Error bars represent the standard deviation (s.d.) of replicate
789 experiments.

790

791 **Acknowledgments**

792 We thank Samuel Rommelaere, Jean-Philippe Boquette, Fanny Schüpfer for
793 experimental help. We thank Kathryn Bushley and Carolyn Elya for providing the
794 *Entomophthora muscae* strains used for this study. Guiqing Liu stay in the Lemaitre lab
795 was supported by funding from the China Scholarship Council (CSC, No.
796 202208440111) and the SNSF grant TMAG-3_225935. This project was supported by
797 the SNSF grants (310030_215073).

798

799 **Author Contributions**

800 Conceived and designed the experiments: GQL BL. Performed the experiments: GQL
801 YT JL. Analyzed the data: GQL BL. Contributed reagents/ materials/analysis tools:
802 MAH BL. Wrote the paper: GQL MAH BL.

803

804 **References**

805 Almaliki HS, Niu M, Keller NP, Yin G, Bennett JW. 2023. Mutational analysis of aspergillus
806 fumigatus volatile oxylipins in a Drosophila eclosion assay. *J Fungi* **9**:402.

807 doi:10.3390/jof9040402
808 Ballou ER, Avelar GM, Childers DS, Mackie J, Bain JM, Wagener J, Kastora SL, Panea MD,
809 Hardison SE, Walker LA, Erwig LP, Munro CA, Gow NAR, Brown GD, MacCallum DM,
810 Brown AJP. 2016. Lactate signalling regulates fungal β-glucan masking and immune evasion.
811 *Nat Microbiol* **2**:16238. doi:10.1038/nmicrobiol.2016.238
812 Binggeli O, Neyen C, Poidevin M, Lemaitre B. 2014. Prophenoloxidase activation is required for
813 survival to microbial infections in Drosophila. *PLoS Pathog* **10**:e1004067.
814 doi:10.1371/journal.ppat.1004067
815 Boucias D, Liu S, Meagher R, Baniszewski J. 2016. Fungal dimorphism in the entomopathogenic
816 fungus Metarhizium rileyi: Detection of an in vivo quorum-sensing system. *J Invertebr Pathol*
817 **136**:100–108. doi:10.1016/j.jip.2016.03.013
818 Brown AJP. 2023. Fungal resilience and host–pathogen interactions: Future perspectives and
819 opportunities. *Parasite Immunol* **45**:e12946. doi:10.1111/pim.12946
820 Buchon N, Poidevin M, Kwon H-M, Guillou A, Sottas V, Lee B-L, Lemaitre B. 2009. A single
821 modular serine protease integrates signals from pattern-recognition receptors upstream of the
822 Drosophila Toll pathway. *Proc Natl Acad Sci* **106**:12442–12447.
823 doi:10.1073/pnas.0901924106
824 Capilla A, Karachentsev D, Patterson RA, Hermann A, Juarez MT, McGinnis W. 2017. Toll pathway
825 is required for wound-induced expression of barrier repair genes in the Drosophila epidermis.
826 *Proc Natl Acad Sci* **114**. doi:10.1073/pnas.1613917114
827 Carboni AL, Hanson MA, Lindsay SA, Wasserman SA, Lemaitre B. 2022. Cecropins contribute to
828 Drosophila host defense against a subset of fungal and Gram-negative bacterial infection.
829 *Genetics* **220**:iyab188. doi:10.1093/genetics/iyab188
830 Carvalho L, Jacinto A, Matova N. 2014. The Toll/NF-κB signaling pathway is required for
831 epidermal wound repair in Drosophila. *Proc Natl Acad Sci* **111**. doi:10.1073/pnas.1408224111
832 Casalini G, Giacomelli A, Antinori S. 2024. The WHO fungal priority pathogens list: a crucial
833 reappraisal to review the prioritisation. *Lancet Microbe* **5**:717–724. doi:10.1016/S2666-
834 5247(24)00042-9
835 Cen K, Li B, Lu Y, Zhang S, Wang C. 2017. Divergent LysM effectors contribute to the virulence
836 of Beauveria bassiana by evasion of insect immune defenses. *PLOS Pathog* **13**:e1006604.
837 doi:10.1371/journal.ppat.1006604
838 Clemmons AW, Lindsay SA, Wasserman SA. 2015. An effector peptide family required for
839 Drosophila Toll-mediated immunity. *PLOS Pathog* **11**:e1004876.
840 doi:10.1371/journal.ppat.1004876
841 Cohen LB, Lindsay SA, Xu Y, Lin SJH, Wasserman SA. 2020. The Daisho peptides mediate
842 Drosophila defense against a subset of filamentous fungi. *Front Immunol* **11**:9.
843 doi:10.3389/fimmu.2020.00009
844 De Fine Licht HH, Jensen AB, Eilenberg J. 2017. Comparative transcriptomics reveal host-specific
845 nucleotide variation in entomophthoralean fungi. *Mol Ecol* **26**:2092–2110.
846 doi:10.1111/mec.13863
847 De Gregorio E. 2002. The Toll and Imd pathways are the major regulators of the immune response
848 in Drosophila. *EMBO J* **21**:2568–2579. doi:10.1093/emboj/21.11.2568
849 Dean R, Van Kan JAL, Pretorius ZA, Hammond-Kosack KE, Di Pietro A, Spanu PD, Rudd JJ,
850 Dickman M, Kahmann R, Ellis J, Foster GD. 2012. The Top 10 fungal pathogens in molecular

plant pathology. *Mol Plant Pathol* **13**:414–430. doi:10.1111/j.1364-3703.2011.00783.x

Dudzic JP, Hanson MA, Iatsenko I, Kondo S, Lemaitre B. 2019. More than black or white: Melanization and Toll share regulatory serine proteases in Drosophila. *Cell Rep* **27**:1050-1061.e3. doi:10.1016/j.celrep.2019.03.101

Edwards S, De Fine Licht HH. 2024. Rearing zombie flies: Laboratory culturing of the behaviourally manipulating fungal pathogen Entomophthora muscae. *MethodsX* **12**:102523. doi:10.1016/j.mex.2023.102523

Ekengren S, Hultmark D. 1999. Drosophila cecropin as an antifungal agent. *Insect Biochem Mol Biol* **29**:965–972. doi:10.1016/S0965-1748(99)00071-5

El Chamy L, Leclerc V, Caldelari I, Reichhart J-M. 2008. Sensing of "danger signals" and pathogen-associated molecular patterns defines binary signaling pathways "upstream" of Toll. *Nat Immunol* **9**:1165–1170. doi:10.1038/ni.1643

Elya C, De Fine Licht HH. 2021. The genus Entomophthora: bringing the insect destroyers into the twenty-first century. *IMA Fungus* **12**:34. doi:10.1186/s43008-021-00084-w

Elya C, Lok TC, Spencer QE, McCausland H, Martinez CC, Eisen M. 2018. Robust manipulation of the behavior of Drosophila melanogaster by a fungal pathogen in the laboratory. *eLife* **7**:e34414. doi:10.7554/eLife.34414

Fehlbaum P, Bulet P, Michaut L, Lagueux M, Broekaert WF, Hetru C, Hoffmann JA. 1994. Insect immunity. Septic injury of Drosophila induces the synthesis of a potent antifungal peptide with sequence homology to plant antifungal peptides. *J Biol Chem* **269**:33159–33163. doi:10.1016/S0021-9258(20)30111-3

Feldman MB, Vyas JM, Mansour MK. 2019. It takes a village: Phagocytes play a central role in fungal immunity. *Semin Cell Dev Biol* **89**:16–23. doi:10.1016/j.semcdb.2018.04.008

Ferrandon D. 1998. A drosomycin-GFP reporter transgene reveals a local immune response in Drosophila that is not dependent on the Toll pathway. *EMBO J* **17**:1217–1227. doi:10.1093/emboj/17.5.1217

Ferreira ÁG, Naylor H, Esteves SS, Pais IS, Martins NE, Teixeira L. 2014. The Toll-Dorsal pathway is required for resistance to viral oral infection in Drosophila. *PLoS Pathog* **10**:e1004507. doi:10.1371/journal.ppat.1004507

Gao Q, Jin K, Ying S-H, Zhang Y, Xiao G, Shang Y, Duan Z, Hu X, Xie X-Q, Zhou G, Peng G, Luo Z, Huang W, Wang B, Fang W, Wang S, Zhong Y, Ma L-J, St. Leger RJ, Zhao G-P, Pei Y, Feng M-G, Xia Y, Wang C. 2011. Genome sequencing and comparative transcriptomics of the model entomopathogenic fungi Metarhizium anisopliae and M. acridum. *PLoS Genet* **7**:e1001264. doi:10.1371/journal.pgen.1001264

Gladieux P, Ropars J, Badouin H, Branca A, Aguileta G, De Vienne DM, Rodríguez De La Vega RC, Branco S, Giraud T. 2014. Fungal evolutionary genomics provides insight into the mechanisms of adaptive divergence in eukaryotes. *Mol Ecol* **23**:753–773. doi:10.1111/mec.12631

Gottar M, Gobert V, Matskevich AA, Reichhart J-M, Wang C, Butt TM, Belvin M, Hoffmann JA. 2006. Dual detection of fungal infections in Drosophila through recognition of microbial structures and sensing of virulence factors **127**:1425–1437.

Hanson M, Westlake H, Bulet P, Lemaitre B. 2025. The antimicrobial and host defense peptides of Drosophila Melanogaster. *Annu Rev Microbiol*.

Hanson MA. 2024. When the microbiome shapes the host: immune evolution implications for

895 infectious disease. *Philos Trans R Soc B Biol Sci* **379**:20230061. doi:10.1098/rstb.2023.0061
896 Hanson MA, Cohen LB, Marra A, Iatsenko I, Wasserman SA, Lemaitre B. 2021. The Drosophila
897 Baramicin polypeptide gene protects against fungal infection. *PLOS Pathog* **17**:e1009846.
898 doi:10.1371/journal.ppat.1009846
899 Hanson MA, Dostálová A, Ceroni C, Poidevin M, Kondo S, Lemaitre B. 2019. Synergy and
900 remarkable specificity of antimicrobial peptides in vivo using a systematic knockout approach.
901 *eLife* **8**:e44341. doi:10.7554/eLife.44341
902 Hanson MA, Grollmus L, Lemaitre B. 2023. Ecology-relevant bacteria drive the evolution of host
903 antimicrobial peptides in Drosophila. *Science* **381**:eadg5725. doi:10.1126/science.adg5725
904 Hedengren M, BengtÅsling, Dushay MS, Ando I, Ekengren S, Wihlborg M, Hultmark D. 1999.
905 Relish, a central factor in the control of humoral but not cellular immunity in Drosophila. *Mol*
906 *Cell* **4**:827–837. doi:10.1016/s1097-2765(00)80392-5
907 Hong S, Sun Y, Sun D, Wang C. 2022. Microbiome assembly on Drosophila body surfaces benefits
908 the flies to combat fungal infections. *iScience* **25**:104408. doi:10.1016/j.isci.2022.104408
909 Hu X, Xiao G, Zheng P, Shang Y, Su Y, Zhang X, Liu X, Zhan S, St. Leger RJ, Wang C. 2014.
910 Trajectory and genomic determinants of fungal-pathogen speciation and host adaptation. *Proc*
911 *Natl Acad Sci* **111**:16796–16801. doi:10.1073/pnas.1412662111
912 Huang J, Lou Y, Liu J, Bulet P, Cai C, Ma K, Jiao R, Hoffmann JA, Liégeois S, Li Z, Ferrandon D.
913 2023. A Toll pathway effector protects Drosophila specifically from distinct toxins secreted by
914 a fungus or a bacterium. *Proc Natl Acad Sci* **120**:e2205140120. doi:10.1073/pnas.2205140120
915 Hughes DP, Andersen SB, Hywel-Jones NL, Himaman W, Billen J, Boomsma JJ. 2011. Behavioral
916 mechanisms and morphological symptoms of zombie ants dying from fungal infection. *BMC*
917 *Ecol* **11**:13. doi:10.1186/1472-6785-11-13
918 Issa N, Guillaumot N, Lauret E, Matt N, Schaeffer-Reiss C, Van Dorsselaer A, Reichhart J-M,
919 Veillard F. 2018. The circulating protease persephone is an immune sensor for microbial
920 proteolytic activities upstream of the Drosophila Toll pathway. *Mol Cell* **69**:539-550.e6.
921 doi:10.1016/j.molcel.2018.01.029
922 Jang I-H, Chosa N, Kim S-H, Nam H-J, Lemaitre B, Ochiai M, Kambris Z, Brun S, Hashimoto C,
923 Ashida M, Brey PT, Lee W-J. 2006. A spätzle-processing enzyme required for toll signaling
924 activation in drosophila innate immunity. *Dev Cell* **10**:45–55.
925 doi:10.1016/j.devcel.2005.11.013
926 Kambris Z, Brun S, Jang I-H, Nam H-J, Romeo Y, Takahashi K, Lee W-J, Ueda R, Lemaitre B.
927 2006. Drosophila immunity: A large-scale in vivo RNAi screen identifies five serine proteases
928 required for toll activation. *Curr Biol* **16**:808–813. doi:10.1016/j.cub.2006.03.020
929 Lai Y, Jiang B, Hou F, Huang X, Ling B, Lu H, Zhong T, Huang J. 2023. The emerging role of
930 extracellular vesicles in fungi: a double-edged sword. *Front Microbiol* **14**:1216895.
931 doi:10.3389/fmicb.2023.1216895
932 Lazzaro BP, Zasloff M, Rolff J. 2020. Antimicrobial peptides: Application informed by evolution.
933 *Science* **368**:eaau5480. doi:10.1126/science.aau5480
934 Lemaitre B, Nicolas E, Michaut L, Reichhart J-M, Hoffmann JA. 1996. The dorsoventral regulatory
935 gene cassette spätzle/toll/cactus controls the potent antifungal response in Drosophila adults.
936 *Cell* **86**:973–983. doi:10.1016/S0092-8674(00)80172-5
937 Levashina EA, Ohresser S, Bulet P, Reichhart J, Hetru C, Hoffmann JA. 1995. Metchnikowin, a
938 Novel Immune-Inducible Proline-Rich Peptide from Drosophila with Antibacterial and

Antifungal Properties. *Eur J Biochem* **233**:694–700. doi:10.1111/j.1432-1033.1995.694_2.x

Levitin A, Whiteway M. 2008. Drosophila innate immunity and response to fungal infections. *Cell Microbiol* **10**:1021–1026. doi:10.1111/j.1462-5822.2008.01120.x

Li M, Meng Q, Zhang H, Ni R, Zhou G, Zhao Y, Wu P, Shu R, Qin Q, Zhang J. 2020. Vegetative development and host immune interaction of Ophiocordyceps sinensis within the hemocoel of the ghost moth larva, Thitarodes xiaojinensis. *J Invertebr Pathol* **170**:107331. doi:10.1016/j.jip.2020.107331

Liu G, Han R, Cao L. 2019. Artificial cultivation of the chinese cordyceps from injected ghost moth larvae. *Environ Entomol* **48**:1088–1094. doi:10.1093/ee/nvz099

Lohse MB, Johnson AD. 2008. Differential Phagocytosis of White versus Opaque Candida albicans by Drosophila and Mouse Phagocytes. *PLoS ONE* **3**:e1473. doi:10.1371/journal.pone.0001473

Lou Y, Zhang B, Zhang Z, Pan Y, Yang J, Li L, Huang J, Yuan Z, Liegeois S, Bulet P, Xu R, Zi L, Ferrandon D. 2025. Distinct Bomanins at the Drosophila 55C locus function in resistance and resilience to infections. *Annu Rev Entomol*.

Lu M, Wei D, Shang J, Li S, Song S, Luo Y, Tang G, Wang C. 2024. Suppression of Drosophila antifungal immunity by a parasite effector via blocking GNBP3 and GNBP-like 3, the dual receptors for β-glucans. *Cell Rep* **43**:113642. doi:10.1016/j.celrep.2023.113642

Ma M, Luo J, Li C, Eleftherianos I, Zhang W, Xu L. 2024. A life-and-death struggle: interaction of insects with entomopathogenic fungi across various infection stages. *Front Immunol* **14**:1329843. doi:10.3389/fimmu.2023.1329843

Marra A, Hanson MA, Kondo S, Erkosar B, Lemaitre B. 2021. Drosophila antimicrobial peptides and lysozymes regulate gut microbiota composition and abundance. *mBio* **12**:e00824-21. doi:10.1128/mBio.00824-21

Melcarne C, Lemaitre B, Kurant E. 2019. Phagocytosis in Drosophila: From molecules and cellular machinery to physiology. *Insect Biochem Mol Biol* **109**:1–12. doi:10.1016/j.ibmb.2019.04.002

Meng Q, Yu H-Y, Zhang H, Zhu W, Wang M-L, Zhang J-H, Zhou G-L, Li X, Qin Q-L, Hu S-N, Zou Z. 2015. Transcriptomic insight into the immune defenses in the ghost moth, Hepialus xiaojinensis, during an Ophiocordyceps sinensis fungal infection. *Insect Biochem Mol Biol* **64**:1–15. doi:10.1016/j.ibmb.2015.06.014

Michel T, Reichhart J-M, Hoffmann JA, Royet J. 2001. Drosophila Toll is activated by Gram-positive bacteria through a circulating peptidoglycan recognition protein. *Nature* **414**:756–759. doi:10.1038/414756a

Moghaddam M-RB, Gross T, Becker A, Vilcinskas A, Rahnamaeian M. 2017. The selective antifungal activity of Drosophila melanogaster metchnikowin reflects the species-dependent inhibition of succinate–coenzyme Q reductase. *Sci Rep* **7**:8192. doi:10.1038/s41598-017-08407-x

Morelli KA, Kerkaert JD, Cramer RA. 2021. Aspergillus fumigatus biofilms: Toward understanding how growth as a multicellular network increases antifungal resistance and disease progression. *PLOS Pathog* **17**:e1009794. doi:10.1371/journal.ppat.1009794

Mpamhanga CD, Kounatidis I. 2024. The utility of Drosophila melanogaster as a fungal infection model. *Front Immunol* **15**. doi:10.3389/fimmu.2024.1349027

Murante D, Hogan DA. 2024. Drivers of diversification in fungal pathogen populations. *PLOS Pathog* **20**:e1012430. doi:10.1371/journal.ppat.1012430

Nam H-J, Jang I-H, You H, Lee K-A, Lee W-J. 2012. Genetic evidence of a redox-dependent

systemic wound response via Hayan Protease-Phenoloxidase system in Drosophila: Redox-modulated systemic wound response. *EMBO J* **31**:1253–1265. doi:10.1038/emboj.2011.476

Pradeu T, Thomma BPHJ, Girardin SE, Lemaitre B. 2024. The conceptual foundations of innate immunity: Taking stock 30 years later. *Immunity* **57**:613–631. doi:10.1016/j.immuni.2024.03.007

Qu S, Wang S. 2018. Interaction of entomopathogenic fungi with the host immune system. *Dev Comp Immunol* **83**:96–103. doi:10.1016/j.dci.2018.01.010

Quintin J, Asmar J, Matskevich AA, Lafarge M-C, Ferrandon D. 2013. The Drosophila Toll pathway controls but does not clear Candida glabrata infections. *J Immunol* **190**:2818–2827. doi:10.4049/jimmunol.1201861

Rao Z, Cao L, Wu H, Qiu X, Liu G, Han R. 2019. Comparative transcriptome analysis of thitarodes armoricanus in response to the entomopathogenic fungi paecilomyces hepiali and ophiocordyceps sinensis. *Insects* **11**:4. doi:10.3390/insects11010004

Reis FCG, Rodrigues ML. 2025. Things you wanted to know about fungal extracellular vesicles (but were afraid to ask). *PLoS Negl Trop Dis* **19**:e0013038. doi:10.1371/journal.pntd.0013038

Ristow LC, Jezewski AJ, Chadwick BJ, Stamnes MA, Lin X, Krysan DJ. 2023. Cryptococcus neoformans adapts to the host environment through TOR-mediated remodeling of phospholipid asymmetry. *Nat Commun* **14**:6587. doi:10.1038/s41467-023-42318-y

Rodrigues ML, May RC, Janbon G. 2024. The multiple frontiers in the study of extracellular vesicles produced by fungi. *Microbes Infect* **26**:105233. doi:10.1016/j.micinf.2023.105233

Rommelaere S, Carboni A, Bada Juarez JF, Boquete J-P, Abriata LA, Teixeira Pinto Meireles F, Rukes V, Vincent C, Kondo S, Dionne MS, Dal Peraro M, Cao C, Lemaitre B. 2024. A humoral stress response protects Drosophila tissues from antimicrobial peptides. *Curr Biol* **34**:1426-1437.e6. doi:10.1016/j.cub.2024.02.049

Rommelaere S, Masson F, Lemaitre B. 2025. From foes to friends: Fundamental and applied insights on insect-microbe interactions in Overview of insect immunity and symbiosis: Interactions and implicationsComprehensive Molecular Insect Science. Elsevier.

Ryckebusch F, Tian Y, Rapin M, Schüpfer F, Hanson MA, Lemaitre B. 2025. Layers of immunity: Deconstructing the Drosophila effector response. *bioRixv*. doi:10.1101/2025.03.28.645959

Schrank A, Vainstein MH. 2010. Metarhizium anisopliae enzymes and toxins. *Toxicon* **56**:1267–1274. doi:10.1016/j.toxicon.2010.03.008

Shan T, Wang Y, Bhattarai K, Jiang H. 2023. An evolutionarily conserved serine protease network mediates melanization and Toll activation Drosophila. *Sci Adv* **9**. doi:10.1126/sciadv.adk2756

Shang J, Tang G, Yang J, Lu M, Wang C-Z, Wang C. 2023. Sensing of a spore surface protein by a Drosophila chemosensory protein induces behavioral defense against fungal parasitic infections. *Curr Biol* **33**:276-286.e5. doi:10.1016/j.cub.2022.11.004

Shang Y, Xiao G, Zheng P, Cen K, Zhan S, Wang C. 2016. Divergent and convergent evolution of fungal pathogenicity. *Genome Biol Evol* **8**:1374–1387. doi:10.1093/gbe/evw082

Siscar-Lewin S, Hube B, Brunke S. 2022. Emergence and evolution of virulence in human pathogenic fungi. *Trends Microbiol* **30**:693–704. doi:10.1016/j.tim.2021.12.013

Soares MP, Teixeira L, Moita LF. 2017. Disease tolerance and immunity in host protection against infection. *Nat Rev Immunol* **17**:83–96. doi:10.1038/nri.2016.136

Tang G, Song S, Shang J, Luo Y, Li S, Wei D, Wang C. 2025. Fungal evasion of Drosophila immunity involves blocking the cathepsin-mediated cleavage maturation of the danger-sensing

protease. *Proc Natl Acad Sci* **122**:e2419343122. doi:10.1073/pnas.2419343122

Unckless RL, Howick VM, Lazzaro BP. 2016. Convergent Balancing Selection on an Antimicrobial Peptide in Drosophila. *Curr Biol* **26**:257–262. doi:10.1016/j.cub.2015.11.063

Uttenweiler-Joseph S, Moniatte M, Lagueux M, Van Dorsselaer A, Hoffmann JA, Bulet P. 1998. Differential display of peptides induced during the immune response of Drosophila: A matrix-assisted laser desorption ionization time-of-flight mass spectrometry study. *Proc Natl Acad Sci* **95**:11342–11347. doi:10.1073/pnas.95.19.11342

Valanne S, Wang J-H, Rämet M. 2011. The Drosophila Toll signaling pathway. *J Immunol* **186**:649–656. doi:10.4049/jimmunol.1002302

Valero-Jiménez CA, Wiegers H, Zwaan BJ, Koenraadt CJM, Van Kan JAL. 2016. Genes involved in virulence of the entomopathogenic fungus Beauveria bassiana. *J Invertebr Pathol* **133**:41–49. doi:10.1016/j.jip.2015.11.011

Vertyporokh L, Hułas-Stasiak M, Wojda I. 2020. Host–pathogen interaction after infection of Galleria mellonella with the filamentous fungus Beauveria bassiana. *Insect Sci* **27**:1079–1089. doi:10.1111/1744-7917.12706

Wang C, Wang S. 2017. Insect pathogenic fungi: Genomics, molecular interactions, and genetic improvements. *Annu Rev Entomol* **62**:73–90. doi:10.1146/annurev-ento-031616-035509

Wang H, Lu Z, Keyhani NO, Deng J, Zhao X, Huang S, Luo Z, Jin K, Zhang Y. 2023. Insect fungal pathogens secrete a cell wall-associated glucanase that acts to help avoid recognition by the host immune system. *PLOS Pathog* **19**:e1011578. doi:10.1371/journal.ppat.1011578

Wang H, Peng H, Li W, Cheng P, Gong M. 2021. The toxins of Beauveria bassiana and the strategies to improve their virulence to insects. *Front Microbiol* **12**:705343. doi:10.3389/fmicb.2021.705343

Weber ANR, Tauszig-Delamasure S, Hoffmann JA, Lelièvre E, Gascan H, Ray KP, Morse MA, Imler J-L, Gay NJ. 2003. Binding of the Drosophila cytokine Spätzle to Toll is direct and establishes signaling. *Nat Immunol* **4**:794–800. doi:10.1038/ni955

Westlake H, Hanson MA, Lemaitre B. 2024. The Drosophila immunity handbook, First. ed. EPFL Press. doi:10.55430/6304tdihva01

Wichadakul D, Kobmoo N, Ingsriswang S, Tangphatsornruang S, Chantasingh D, Luangsa-ard JJ, Eurwilaichitr L. 2015. Insights from the genome of Ophiocordyceps polyrhachis-furcata to pathogenicity and host specificity in insect fungi. *BMC Genomics* **16**:881. doi:10.1186/s12864-015-2101-4

Xu R, Lou Y, Tidu A, Bulet P, Heinekamp T, Martin F, Brakhage A, Li Z, Liégeois S, Ferrandon D. 2023. The Toll pathway mediates Drosophila resilience to Aspergillus mycotoxins through specific Bomanins. *EMBO Rep* **24**:e56036. doi:10.15252/embr.202256036

Yassine H, Kamareddine L, Osta MA. 2012. The mosquito melanization response is implicated in defense against the entomopathogenic fungus Beauveria bassiana. *PLoS Pathog* **8**:e1003029. doi:10.1371/journal.ppat.1003029

Yuan Y, Huang W, Chen K, Ling E. 2020. Beauveria bassiana ribotoxin inhibits insect immunity responses to facilitate infection via host translational blockage. *Dev Comp Immunol* **106**:103605. doi:10.1016/j.dci.2019.103605

1070 **Figure Legends**
1071
1072 **Figure 1**. **Contribution of the four main immune modules to survival upon natural**
1073 **infection with the five fungi.** (A-E) Survival rate of male wild-type and deficient flies
1074 following infection with the five different fungi shows that *spz*^{rm7} flies (P<0.0001) and
1075 *PPO1*$^{\Delta}$, *PPO2*$^{\Delta}$ flies (P<0.0001) are severely affected in their capacity to survive
1076 infection with the five fungi compared to wild-type flies. (F) Flies that are devoid of all
1077 the four immune modules (*ΔITPM*) have a significantly shorter lifespan (χ^2=78.50,
1078 P<0.0001). Insects treated with 0.05% Tween 80 were used as mock controls. Data were
1079 analyzed by Log-rank test and values are pooled from at least three independent
1080 experiments. Full statistical details are available on Tables S2 and S8.
1081
1082 **Figure 2. Contribution of the four main immune modules to survival upon septic**
1083 **infection with the five fungi.** (**A-C**) Survival rate of male wild-type and deficient flies
1084 following pricking with spore suspensions show that *spz*^{rm7} flies (P<0.0001) contribute
1085 most to resisting infection by the *B. bassiana*, *M. anisopliae*, and *M. rileyi* as that of
1086 natural infection. (**D**) Survival rate of male wild-type and deficient flies following
1087 pricking with spore suspensions show that *spz*^{rm7} and to a lower extent *Rel*^{E20} flies
1088 exhibited a strong susceptibility to infection with *A. fumigatus* (P<0.0001). (**E**) No
1089 significant difference in survival of the four main modules upon infection with *E.*
1090 *muscae* by the injection of protoplasts compared to wild-type flies. (**F**) Survival rate of
1091 male flies following injury with a clean needle show that *PPO1*$^{\Delta}$, *PPO2*$^{\Delta}$ flies are
1092 severely affected in their capacity to survive wounding compared to wild-type flies
1093 (χ^2=20.30, P<0.0001). There was no significant difference in survival of *ΔITPM* flies
1094 upon injection with *E. muscae* protoplasts and injury with a clean needle (χ^2=2.045,
1095 P=0.1527). Data were analyzed by Log-rank test and values are pooled from at least
1096 three independent experiments. Full statistical details are available on Tables S3 and S8.
1097
1098 **Figure 3. The induction of the Toll pathway in wild-type flies upon infection with**
1099 **the five fungi.**
1100 (**A-E**) Expression of *Drosomycin* (*Drs*) in wild-type flies upon natural infection with
1101 the five fungi. Shown are the relative expression levels of *Drs* in relation to Rp49. *B.*
1102 *bassiana*, *M. anisopliae* and *M. rileyi* induced relatively high *Drs* expression (compare
1103 Y axis to F). *A. fumigatus* did not induce *Drs* expression, while *E. muscae* induced a
1104 low *Drs* expression level. (**F**) A high induction of *Drs* was observed in unchallenged
1105 flies and flies 48 h after natural infection with *E. muscae* upon septic injury with the
1106 Gram-positive bacterium *M. luteus*. UC = Unchallenged, CI = Clean Injury, EM =
1107 naturally-infected with *E. muscae;* (**G**) Stronger GFP signal intensity was observed in
1108 flies carrying the *Drs-GFP* reporter gene upon natural infection with *B. bassiana* than
1109 that with *E. muscae*. (**H**) Kinetic analysis of Toll pathway activity was monitored using
1110 unchallenged *Drs-GFP* flies and flies 48 h after natural infection with *E. muscae* upon
1111 septic injury with the Gram-positive bacterium *M. luteus.* (**I**) Septic injury with *B.*
1112 *bassiana* spores induced higher *Drs* expression than natural infection (Compare I to A).
1113 UC = Unchallenged, CI = Clean injection, Bb = *B. bassiana* infection (**J**) Injection with

1114 *E. muscae* protoplasts did not induce *Drs* expression (Compare J to E). UC =
1115 Unchallenged, PBS = Sterile injection, Em = *E. muscae* injection. (**K**) Stronger GFP
1116 intensity was observed in flies carrying the *Drs-GFP* reporter gene upon septic
1117 infection with *B. bassiana* than that with *E. muscae*. Expression was normalized with
1118 w^{1118} UC set as a value of 1. Data were analyzed using One-Way ANOVA followed by
1119 Tukey's multiple comparison tests. Values represent the mean ± s.d. of at least three
1120 independent experiments. ns, P>0.05, *, P<0.05; **, P<0.01; ***, P<0.001. Full
1121 statistical details are available on Table S8.
1122
1123 **Figure 4. Morphological development of *E. muscae in vitro* culture and in flies.** (**A**)
1124 The morphological development of *E. muscae* protoplasts in Grace's Insect Medium
1125 showed that round protoplast sprouted and extended to grow at the site of vesicles to
1126 form hyphae. Calcofluor White M2R staining showed that cell wall is only present
1127 when protoplasts have transformed to hyphae. V: vesicle. (**B**) Five infection stages of
1128 *E. muscae* were defined based on the morphological change of flies after infection. Red
1129 arrows indicate the white abdomen. (**C**) Calcofluor White M2R staining showed the
1130 presence of cell wall of spores contacting with host cuticle (S1), the absence of cell wall
1131 of protoplasts (S2), and the presence of thin cell wall when protoplasts transformed to
1132 invasive hyphae at S3-S4 and hyphae S5. Red arrows indicate the presence of vesicle
1133 in protoplasts and hyphae. C: cuticle; White arrows indicate the primary conidia
1134 produced at the tip of the hyphae that extrude from the cadavers.
1135
1136 **Figure 5. Contribution of the Psh and GNBP3 to Toll pathway activation.** (**A**) A
1137 model of GNBP3 and SPs regulating the Toll pathway and the Melanization reaction
1138 upon fungal infections. (**B-E**) Natural infection with *B. bassiana*, *M. anisopliae*, and *M.*
1139 *rileyi* revealed that psh^{SK1} flies have a reduced survival rate compared to $GNBP3^{hades}/Df$
1140 *(ED4421)*, $modSP^{1}$ and wild-type flies (P<0.0001). $modSP^{1}$ flies were as susceptible to
1141 *E. muscae* as spz^{rm7} and psh^{1} flies (P>0.05). The Hayan-psh^{Def} double mutant flies is
1142 more susceptible to *B. bassiana*, *M. anisopliae* and *M. rileyi* than psh^{SK1} (Bb, χ^2=36.19,
1143 P<0.0001; Ma, χ^2=16.91, P<0.0001; Mr, χ^2=14.14, P=0.0002). Likewise, the double
1144 mutant flies *psh;;modSP* were more susceptible to *B. bassiana*, *M. anisopliae* and *M.*
1145 *rileyi* than psh^{SK1} (Bb, χ^2=14.65, P=0.0001; Ma, χ^2=54.88, P<0.0001; Mr, χ^2=22.68,
1146 P<0.0001) and $modSP^{1}$ (Bb, χ^2=173.1, P<0.0001; Ma, χ^2=120.6, P<0.0001; Mr,
1147 χ^2=55.81, P<0.0001). (**F**) Expression of *Drs* revealed that $GNBP3^{hades}$ flies have wild-
1148 type *Drs* expression levels (p>0.05). The Toll pathway was not activated in psh^{SK1} flies
1149 as in spz^{rm7}, psh^{1} and *Hayan-psh* ^{Def} flies, and displayed a lower induction in $modSP^{1}$
1150 flies compared to wild-type flies. (**G**) Expression of *BomBc3* showed similar results to
1151 the expression of *Drs*. The spz^{rm7} flies as a positive control. Survival tests were analyzed
1152 by Log-rank test and gene expression data were analyzed using One-Way ANOVA
1153 followed by Tukey's multiples comparison tests. Values represent the mean ± s.d. of at
1154 least three independent experiments. Full statistical details are available on Tables S4
1155 and S8.
1156
1157 **Figure 6. Higher fungal persistence in flies deficient for the Toll pathway**. (**A-C**)

1158 Quantification of fungal loads by qPCR analyses reveals higher fungal loads in *spz*^{rm7}
1159 flies compared to wild-type flies after natural infection with *B. bassiana*, *M. anisopliae*
1160 and *E. muscae*. (**D-E**) Higher proportion of flies with GFP and a stronger GFP intensity
1161 were observed in *spz*^{rm7} flies compared to wild-type flies at 48, 72 and 96 hours after
1162 pricking with spores of a *M. anisopliae* tagged GFP strain. ns, P>0.05, **, P<0.01; ****,
1163 P<0.0001. Full statistical details are available on Table S8.
1164
1165 **Figure 7. Contribution of host defense peptides and Serine Proteases involved in**
1166 **melanization to survival upon fungal infection.** (**A**) The Bomanin and Daisho1/2 are
1167 critical for defense against *B. bassiana*, *M. anisopliae*, *M. rileyi* and *E. muscae* infection.
1168 (**B**) PPO2 mutant flies were more susceptible to fungal infection than PPO1. The *spz*^{rm7}
1169 flies as a positive control. Shown are the median survival for infection with *B. bassiana*,
1170 *M. anisopliae* and *E. muscae*, and cumulative survival for infection with *M. rileyi*. Data
1171 were analyzed using the Log rank test. ns, P>0.05; *, p<0.05; ***, P<0.001; ****,
1172 P<0.0001. Full statistical details are available on Tables S5-6 and S8.
1173
1174 **Figure 8. Melanization limits fungal growth.** (**A**) *B. bassiana* fungal load increases
1175 in wild-type and mutants before mortality upon natural infection. *spz*^{rm7} and *PPO1*$^{\triangle}$,
1176 *PPO2*$^{\triangle}$ flies have a higher fungal persistence in *PPO1*$^{\triangle}$, *PPO2*$^{\triangle}$ flies. (**B**) *M.*
1177 *anisopliae* fungal load increases in wild-type and mutants showing similar trends as *B.*
1178 *bassiana* fungal load before mortality upon natural infection. Data were analyzed using
1179 One-Way ANOVA followed by Tukey's multiples comparison tests and values are
1180 pooled data from three independent experiments. (**C**) Stronger GFP intensity and faster
1181 fungal dissemination was observed in *spz*^{rm7} and *PPO1*$^{\triangle}$, *PPO2*$^{\triangle}$ flies upon pricking
1182 with spores of a *M. anisopliae* tagged GFP strain. Red arrow indicates the growth of
1183 hyphae at the melanization spot of the pricking site. Full statistical details are available
1184 on Table S8.

Supplementary Material

Table S1 List of wild-type and mutant flies used in this study.

***Drosophila* lines**	**Source**	**Abbrevation**
iso; PPO1$^{\Delta}$; iso	Binggeli et al., 2014	*PPO1$^{\Delta}$*
iso; PPO2$^{\Delta}$; iso	Binggeli et al., 2014	*PPO2$^{\Delta}$*
iso; PPO1$^{\Delta}$, PPO2$^{\Delta}$; iso	Binggeli et al., 2014	*PPO1$^{\Delta}$, PPO2$^{\Delta}$*
iso; iso; Rel^{E20}	Hedengren et al., 1999	*Rel^{E20}*
iso; iso; spz^{rm7}	Lemaitre et al., 1996	*spz^{rm7}*
+; Nim C1^{1}; Eater^{1}	Melcarne et al., 2019	*Nim C1^{1}; Eater^{1}*
iso (Hayan-psh)^{Def}; NimC1^{1}; Eater1, Relish^{E20}	Ryckebusch et al., 2025	*ΔITPM*
Hayan^{SK6}; iso; iso	Duzic et al., 2019	*Hayan^{SK6}*
psh^{SK1}; iso; iso	Duzic et al., 2019	*psh^{SK1}*
Hayan-psh^{Def}; iso; iso	Duzic et al., 2019	*Hayan-psh^{Def}*
+; +; GNBP3Δ40/TM6B	Gottar et al., 2006	*GNBP3^{hades}*
iso; iso; GNBP3Δ	Lu et al., 2024	*GNBP3$^{\Delta}$*
iso; GNBP like 3Δ; iso	Lu et al., 2024	*GL3$^{\Delta}$*
iso; GNBP like 3Δ;GNBP3Δ	Lu et al., 2024	*G3$^{\Delta}$;GL3$^{\Delta}$*
w[1118];Df(3L)ED4421,P{w[+mW.ScerFRT.hs3]	BDSC#8066	*ED4421^{Def}*
iso; iso; Sp7^{SK6}	Duzic et al., 2019	*Sp7^{SK6}*
iso; iso; modSP^{1}	Buchon et al., 2009	*modSP^{1}*
Psh^{1}; iso; modSP^{1}	Buchon et al., 2009	*psh^{1};; modSP^{1}*
iso; Mtk^{R1}; iso	Hanson et al., 2019	*Mtk^{R1}*
iso; iso; Drs^{R1}	Hanson et al., 2019	*Drs^{R1}*
iso; Bom[Δ55C-289]; iso	Clemmons et al., 2015	*Bom$^{\Delta 55C}$*
iso; BaraAΔ{dsRed}; iso	Hanson et al., 2021	*BaraA$^{\Delta}$*
iso; ΔAMP10	Caboni et al., 2022	*ΔAMP10*
iso; ΔAMP14	Caboni et al., 2022	*ΔAMP14*
iso; ΔDaisho 1,2; iso	Cohen et al., 2020	*ΔDso*
iso; Mtk^{R1}; Drs^{R1}	Hanson et al., 2021	*Mtk^{R1}; Drs^{R1}*
iso; BaraA^{SW1}, ΔDso; iso	Bruno Lemaitre	*BaraA$^{\Delta}$, ΔDso*
iso; Mtk^{R1}, BaraA^{SW1}; DrsR1	Bruno Lemaitre	*Mtk^{R1},BaraA$^{\Delta}$; Drs^{R1}*

iso; Mtk^{R1}, BaraA^{SW1}, ΔDso; DrsR1	Bruno Lemaitre	*Mtk^{R1},BaraA^{Δ},ΔDso; Drs^{R1}*
iso; Mtk^{R1}, Bom^{Δ55C}; Drs^{R1}	Bruno Lemaitre	*Mtk^{R1}, Bom^{Δ55C}; Drs^{R1}*

1187

1188 **Table S2 Survival analyses in flies deficient for individual or combinations of the**

1189 **four immune modules upon topical infection of the five fungi. Related to Figure 1.**

Fungal species	Flies	LT_{50} (days)	χ^{2*}	P value (vs w^{1118})
B. bassiana	*w^{1118}*	undefined	-	-
	OR-R	undefined	0.1571	0.6918
	Rel^{E20}	14	2.224	0.1359
	spz^{rm7}	3	97.74	<0.0001
	ΔITPM	3	76.40	<0.0001
	PPO1^{Δ}, PPO2^{Δ}	5.5	63.04	<0.0001
	NimC$_1^1$; Eater^1	14	1.892	0.1689
M. anisopliae	*iso w^{1118}*	6.5	-	-
	OR-R	9	0.3653	0.5456
	Rel^{E20}	6	3.826	0.0505
	spz^{rm7}	4	60.77	<0.0001
	ΔITPM	3	78.33	<0.0001
	PPO1^{Δ}, PPO2^{Δ}	5	22.34	<0.0001
	NimC$_1^1$; Eater^1	8	0.08859	0.7660
M. rileyi	*w^{1118}*	undefined	-	-
	OR-R	undefined	0.0001	0.9983
	Rel^{E20}	undefined	1.270	0.2598
	spz^{rm7}	4	183.1	<0.0001
	ΔITPM	13	220.6	<0.0001
	PPO1^{Δ}, PPO2^{Δ}	4	17.86	<0.0001
	NimC$_1^1$; Eater^1	undefined	1.949	0.1627
A. fumigatus	*w^{1118}*	undefined	-	-
	OR-R	undefined	0.0121	0.9123
	Rel^{E20*1}	undefined	4.407	0.0358
	spz^{rm7}	13	103.4	<0.0001
	ΔITPM	7	184.2	<0.0001
	PPO1^{Δ}, PPO2^{Δ}	undefined	18.68	<0.0001
	NimC$_1^1$; Eater^1	undefined	1.964	0.1610
E. muscae	*w^{1118}*	8	-	-
	Canton S	7	1.197	0.2740
	Rel^{E20}	9	0.3641	0.5463
	spz^{rm7}	4	121.3	<0.0001
	ΔITPM	4	117.2	<0.0001
	PPO1^{Δ}, PPO2^{Δ}	6	21.49	<0.0001

	NimC$_1^1$; Eater^1	7	0.2330	0.6293
Mock	*w^{1118}*	undefined		
	Canton S	undefined	0.9825	0.3216
	Rel^{E20}	undefined	6.519	0.0107
	spz^{rm7}	undefined	1.023	0.3119
	ΔITPM	9	78.50	<0.0001
	PPO1$^{\Delta}$, PPO2$^{\Delta}$	undefined	6.516	0.0107
	NimC$_1^1$; Eater^1	undefined	3.627	0.0569

* Note: Survival and log-rank tests were conducted in batch between WT and individual mutants for more than three independent experiments. The null mutant flies were highlighted in bold for showing significant susceptibility (P<0.05) in reference to the WT.

*1: *Rel^{E20}* flies were more susceptible to *A. fumigatus* than *w^{1118}* is not due to *A. fumigatus*, since no significant difference were found between the flies challenged with *A. fumigatus* and unchallenged flies (χ^2=1.448, P=0.2289).

Table S3 Survival analyses in flies deficient for individual or combinations of the four immune modules upon septic infection of the five fungi. Related to Figure 2.

Fungal species	Flies	LT_{50} (days)	χ^{2*}	P value (vs w^{1118})
B. bassiana	*w^{1118}*	6	-	-
	Rel^{E20}	5	0.0061	0.9375
	spz^{rm7}	3	74.36	<0.0001
	ΔITPM	3	114.2	<0.0001
	PPO1$^{\Delta}$, PPO2$^{\Delta}$	5	4.341	0.0372
	NimC$_1^1$; Eater^1	6	0.0029	0.9572
M. anisopliae	*w^{1118}*	5	-	-
	Rel^{E20}	4	0.2045	0.6511
	spz^{rm7}	3	70.32	<0.0001
	ΔITPM	3	41.79	<0.0001
	PPO1$^{\Delta}$, PPO2$^{\Delta}$	5	0.0003	0.9867
	NimC$_1^1$; Eater^1	4	1.337	0.2476
M. rileyi	*w^{1118}*	undefined	-	-
	Rel^{E20}	undefined	0.5389	0.4629
	spz^{rm7}	4	60.61	<0.0001
	ΔITPM	4	74.19	<0.0001
	PPO1$^{\Delta}$, PPO2$^{\Delta}$	undefined	2.736	0.0981
	NimC$_1^1$; Eater^1	undefined	3.504	0.0612
A. fumigatus	*w^{1118}*	undefined	-	-
	Rel^{E20}	7	86.31	<0.0001
	spz^{rm7}	5	95.43	<0.0001
	ΔITPM	5	102.6	<0.0001
	PPO1$^{\Delta}$, PPO2$^{\Delta}$	undefined	3.645	0.0562
	NimC$_1^1$; Eater^1	undefined	1.752	0.1856
E. muscae	*w^{1118}*	6	-	-
	Rel^{E20}	7	1.004	0.3163

	spz^{rm7}	6	3.527	0.0604
	ΔITPM	5	9.986	0.0016
	PPO1$^{\Delta}$, PPO2$^{\Delta}$	6	1.887	0.1696
	NimC$_1^1$; Eater^1	6	0.005028	0.9435
Clean injury	*w^{1118}*	Undefined		
	Rel^{E20}	Undefined	5.438	0.0197
	spz^{rm7}	Undefined	0.2075	0.6487
	ΔITPM	5	112.5	<0.0001
	PPO1$^{\Delta}$, PPO2$^{\Delta}$	Undefined	20.30	<0.0001
	NimC$_1^1$; Eater^1	Undefined	2.231	0.1353

1197 * Note: Survival and log-rank tests were conducted in batch between WT and individual mutants for
1198 at least three independent experiments. The null mutant flies were highlighted in bold for showing
1199 significant susceptibility (P<0.05) in reference to the WT.

1200 **Table S4 Survival analyses in flies deficient for the two upstream pathways activating Toll**
1201 **pathway upon natural infection. Related to Figure 5.**

Fungal species	Flies	LT$_{50}$ (days)	χ^{2*}	P value (vs w^{1118})
B. bassiana	*w^{1118}*	12.5	-	-
	GNBP3^{hades}/Df(ED4421)	9	9.254	0.0024
	modSP^1	10	6.821	0.0090
	psh^{SK1}	5	142.1	<0.0001
	spz^{rm7}	5	129.6	<0.0001
	Hayan-psh^{Def}	4	214.7	<0.0001
	Psh^1;;modSP^1	4	192.9	<0.0001
M. anisopliae	*w^{1118}*	7	-	-
	GNBP3^{hades}/Df(ED4421)	7	5.594	0.018
	modSP^1	7	5.518	0.0188
	psh^{SK1}	5	57.46	<0.0001
	spz^{rm7}	4	103.2	<0.0001
	Hayan-psh^{Def}	4	77.24	<0.0001
	Psh^1;;modSP^1	4	128.1	<0.0001
M. rileyi	*w^{1118}*	undefined		-
	GNBP3^{hades}/Df(ED4421)	undefined	5.678	0.0172
	modSP^1	undefined	5.978	0.0145
	psh^{SK1}	10.5	68.42	<0.0001
	spz^{rm7}	7	122.5	<0.0001
	Hayan-psh^{Def}	7	149.2	<0.0001
	Psh^1;;modSP^1	6	171.0	<0.0001
E. muscae	*w^{1118}*	7		-

	GNBP3^{hades}/Df(ED4421)	7	0.1978	0.6565
	modSP^{1}	5	62.98	<0.0001
	psh^{SK1}	5	63.98	<0.0001
	spz^{rm7}	5	87.33	<0.0001
	Hayan-psh^{Def}	5	66.80	<0.0001
	Psh^{1};;modSP^{1}	5	70.06	<0.0001

1202 * Note: Survival and log-rank tests were conducted in batch between WT and individual mutants for
1203 at least three independent experiments. The null mutant flies were highlighted in bold for showing
1204 significant susceptibility (P<0.05) in reference to the WT.

1205 **Table S5 Survival analyses in flies deficient for individual or combinations of the AMPs upon**
1206 **natural infection of the four entomopathogenic fungi. Related to Figure 7A.**

Fungal species	Flies	LT_{50} (days)	χ^{2*}	P value
B. bassiana	*w^{1118}*	14	-	-
	OR-R	undefined	1.624	0.2025
	spz^{rm7}	4	79.55	<0.0001
	Bom$^{\Delta 55C}$	5	38.62	<0.0001
	Mtk	undefined	1.337	0.2475
	BaraA$^{\Delta}$	9	4.904	0.0268
	Drs	9.5	0.8523	0.3559
	$^{\Delta}$Dso	10	4.179	0.0409
	$^{\Delta}$AMP10	14	0.0021	0.9638
	$^{\Delta}$AMP14	9	3.954	0.468
	Mtk^{R1}; Drs^{R1}	11	0.8154	0.3665
	BaraA$^{\Delta}$, $^{\Delta}$Dso	7	10.02	0.0010
	Mtk^{R1}, BaraA$^{\Delta}$; Drs^{R1}	10	4.472	0.0294
	Mtk^{R1}, Bom$^{\Delta 55C}$; Drs^{R1}	5	61.11	<0.0001
	Mtk^{R1}, BaraA$^{\Delta}$, $^{\Delta}$Dso; Drs^{R1}	7	12.41	0.0004
M. anisopliae	*w^{1118}*	6	-	-
	OR-R	9	0.2458	0.6201
	spz^{rm7}	4	76.12	<0.0001
	Bom$^{\Delta 55C}$	5	32.35	<0.0001
	Mtk	8	0.1939	0.6597
	BaraA$^{\Delta}$	6	6.369	0.0116
	Drs	7	1.391	0.2382
	$^{\Delta}$Dso	6	10.31	0.0013
	$^{\Delta}$AMP10	10	0.5140	0.4734
	$^{\Delta}$AMP14	6	6.043	0.0140
	Mtk^{R1}; Drs^{R1}	6	3.297	0.0694
	BaraA$^{\Delta}$, $^{\Delta}$Dso	6	11.10	0.0009

	Mtk^{R1}, BaraA$^{\Delta}$; Drs^{R1}	6	10.14	0.0015
	Mtk^{R1}, Bom$^{\Delta 55C}$; Drs^{R1}	4	52.43	<0.0001
	Mtk^{R1}, BaraA$^{\Delta}$, $^{\Delta}$Dso; Drs^{R1}	5	11.92	0.0006
M. rileyi	*w^{1118}*	undefined	-	-
	OR-R	undefined	0.3856	0.5346
	spz^{rm7}	11	72.74	<0.0001
	Bom$^{\Delta 55C}$	undefined	28.39	<0.0001
	Mtk	undefined	0.1206	0.7284
	BaraA$^{\Delta}$	undefined	0.04555	0.8310
	Drs	undefined	0.6622	0.4158
	$^{\Delta}$Dso	undefined	14.96	0.0001
	$^{\Delta}$AMP10	undefined	0.3144	0.5750
	$^{\Delta}$AMP14	undefined	2.207	0.1374
	Mtk^{R1}; Drs^{R1}	undefined	0.5849	0.4444
	BaraA$^{\Delta}$, $^{\Delta}$Dso	undefined	19.95	<0.0001
	Mtk^{R1}, BaraA$^{\Delta}$; Drs^{R1}	undefined	4.723	0.0298
	Mtk^{R1}, Bom$^{\Delta 55C}$; Drs^{R1}	12	48.84	<0.0001
	Mtk^{R1}, BaraA$^{\Delta}$, $^{\Delta}$Dso; Drs^{R1}	undefined	27.43	<0.0001
E.muscae	*w^{1118}*	9	-	-
	Canton S	7	1.378	0.2405
	spz^{rm7}	5	134.6	<0.0001
	Bom$^{\Delta 55C}$	6	63.14	<0.0001
	Mtk	8	0.9179	0.3380
	BaraA$^{\Delta}$	7.5	2.543	0.1108
	Drs	10	2.702	0.1002
	$^{\Delta}$Dso	7	12.26	0.0005
	$^{\Delta}$AMP10	8	0.006060	0.9379
	$^{\Delta}$AMP14	8	1.031	0.3100
	Mtk^{R1}; Drs^{R1}	9	1.897	0.1684
	BaraA$^{\Delta}$, $^{\Delta}$Dso	6	22.02	<0.0001
	Mtk^{R1}, BaraA$^{\Delta}$; Drs^{R1}	8	0.001858	0.9656
	Mtk^{R1}, Bom$^{\Delta 55C}$; Drs^{R1}	6	57.14	<0.0001
	Mtk^{R1}, BaraA$^{\Delta}$, $^{\Delta}$Dso; Drs^{R1}	6	21.93	<0.0001

[*] Note: Survival and log-rank tests were conducted in batch between WT and individual mutants for at least three independent experiments. The null mutant flies were highlighted in bold for showing significant susceptibility (P<0.05) in reference to the WT.

1211 **Table S6 Survival analyses in flies deficient for individual or combination of the melanization**

1212 **pathway upon nature infection with the four entomopathogenic fungi. Related to Figure 7B.**

Fungal species	Flies	LT_{50} (days)	χ^{2*}	P value
B. bassiana	w^{1118}	5	-	-
	PPO1$^{\triangle}$	6	3.148	0.0760
	PPO2$^{\triangle}$	3	4.411	0.0357
	spz^{rm7}	3	182.4	<0.0001
	Hayan^{SK6}	6	1.611	0.2043
	Sp7^{SK6}	6	4.600	0.0320
	PPO1$^{\triangle}$***, PPO2***$^{\triangle}$	5	34.73	<0.0001
M. anisopliae	w^{1118}	6	-	-
	PPO1$^{\triangle}$	6	0.1147	0.7349
	PPO2$^{\triangle}$	6	5.287	0.0215
	spz^{rm7}	4	70.42	<0.0001
	Hayan^{SK6}	6	4.270	0.0388
	Sp7^{SK6}	6	4.417	0.0356
	PPO1$^{\triangle}$***, PPO2***$^{\triangle}$	5	26.55	<0.0001
M. rileyi	w^{1118}	Undefined	-	-
	PPO1$^{\triangle}$	Undefined	1.097	0.2949
	PPO2$^{\triangle}$	Undefined	0.8972	0.3435
	spz^{rm7}	7	138.7	<0.0001
	Hayan^{SK6}	Undefined	0.04354	0.8347
	Sp7^{SK6}	Undefined	0.1618	0.6875
	PPO1$^{\triangle}$***, PPO2***$^{\triangle}$	Undefined	20.90	<0.0001
E. muscae	w^{1118}	7	-	-
	PPO1$^{\triangle}$	8	3.146	0.0761
	PPO2$^{\triangle}$	6	4.281	0.0386
	spz^{rm7}	4	106.5	<0.0001
	Hayan^{SK6}	6	6.405	0.0114
	Sp7^{SK6}	7	0.02832	0.8664
	PPO1$^{\triangle}$***, PPO2***$^{\triangle}$	5	39.64	<0.0001

1213 * Note: Survival and log-rank tests were conducted in batch between WT and individual mutants for

1214 at least three independent experiments. The null mutant flies were highlighted in bold for showing

1215 significant susceptibility (P<0.05) in reference to the WT.

Table S7 Primers used in this study.

Genes	Primers	Primer sequencs (5'-3')	Application	Source
Fly GNBP3	G3-F	TGGCGTTCAGGGGTATGAAG	Identify GNBP3 mutant	Lemaitre lab
	G3-R	CGTCTTCGCGATAACCCAGT		
Fly *Drs*	Drs_F	CGTGAGAACCTTTTCCAATATGAT	RT-PCR/qPCR	Lemaitre lab
	Drs_R	TCCCAGGACCACCAGCAT		
Fly *BomBc3*	BomBc3_F	CTGATCGGCGCTCATCCCAG	RT-PCR/qPCR	Lemaitre lab
	BomBc3_R	GGGATGAGGAGAAGCTGCGG		
Fly *Rp49*	Rp49_F	GCCGCTTCAAGGGACAGTATCTG	RT-PCR/qPCR	Lemaitre lab
	Rp49_R	AAACGCGGTTCTGCATGAG		
B. bassiana 18S rRNA	Bbas_18S_F	CGGGTAACGGAGGGTTAGG	Detection of fungal burden by qPCR	Hasan et al., 2021
	Bbas_18S_R	AGTACACGCGGTGAGGCGG		
Fly *actin*	Act-F	GCCAACCGTGAGAAGATGA	Detection of fungal burden by qPCR	Shang et al., 2023
	Act-R	GGTGGTGAAAGAGTAACCGC		
M. anisopliae Rpl32	Rpl-F	ATCGGTTTCGGGTCCAAC		
	Rpl-R	ATTCGCTTTCGGGAGGAG		
E. muscae 18SrRNA	Emus_18S_F	CGGGTGACGGGGAATAAGG	Detection of fungal burden by qPCR	Bruno Lemaitre lab
	Emus_18S_R	GCCAAGAACTGAAACTAACCC		

Figure S1. Survival of the female wild-type and mutant flies deficient for the four main immune modules upon natural infection with the five fungi. (**A-E**) Survival rate of the females shows that *spz*^{rm7} flies (P<0.0001) and *PPO1, PPO2* double mutant flies (P<0.0001) are severely affected in their capacity to survive infection with the five fungi compared to wild-type *w*^{1118} flies. (**F**) The evaluation of spore concentration after the 24 h ejection from the fresh cadavers shows that more spores were produced from female cadavers than male cadavers (**, P<0.01). For natural infection of *E. muscae*, a total of 10 female and 10 male fresh cadavers were used for one infection treatment by spore shower. Data were analyzed using the Log rank test and values are pooled data from at least three independent experiments. Full statistical details are available on Table S8. Related to Figure 1.

Figure S2. Survival of the female wild-type and mutants devoid of the four main immune modules upon septic infection with the five fungi. (**A-C**) Survival rate of females following pricking with spore suspensions show that *spz*^{rm7} flies (P<0.0001) contribute most to resisting infection by the *B. bassiana*, *M. anisopliae*, and *M. rileyi*. (**D**) *spz*^{rm7} and to lower extent *Rel*^{E20} females exhibited a strong susceptibility to infection with *A. fumigatus* (P<0.0001). (**E**) No significant difference in survival of the four main modules upon infection with *E. muscae* by the injection of protoplasts compared to wild-type females. (**F**) Survival of *w*^{1118} flies upon infection with *E. muscae* showed that faster killing was found when injected with a higher concentration of protoplasts (****, P<0.0001). Data were analyzed using the Log rank test and values

are pooled data from at least three independent experiments. Full statistical details are available on Table S8. Related to Figure 2.

Figure S3. Expression of Bomanin (*BomBc3*) in wild-type flies upon infection with the five fungi. (**A-C**) Natural infection with *M. anisopliae* induced a highest expression of *BomBc3,* followed by *B. bassiana* and *M. rileyi* only induced the expression of *BomBc3* at a late stage, at 120 h after infection. (**D**) Natural infection with *A.fumigatus* could not induce the expression of *BomBc3.* (**E**) Natural infection with *E. muscae* induced a low expression of *BomBc3* at 24 h and 48 h after infection, then followed by a significant decrease. (**F**) Septic infection with *B. bassiana* spores activates higher *BomBc3* expression compared to natural infection and clean injury with a needle. (**G**) Expression of *BomBc3* after injection with *E. muscae* protoplasts was similar to the injection with PBS, indicating protoplasts cannot activate Toll signaling. Expression was normalized with w^{1118} UC set as a value of 1. Data were analyzed using One-Way ANOVA followed by Tukey's multiple comparison tests. ns, P>0.05; *, P<0.05; **, P<0.01; ***, P<0.001; ****, P<0.0001. Values represent the mean ± s.d. of at least three independent experiments. Full statistical details are available on Table S8. Related to Figure 3.

Figure S4. DAPI staining of the *E. muscae* protoplasts.

Figure S5. Contribution of GNBP3 and GNGP like 3 to survival upon natural infection with *B. bassiana* and *M. anisopliae*. (**A-B**) Survival rate of male flies following infection with the two fungi shows that both GNBP3 and GNGP like 3 mutant flies are not susceptible or slightly susceptible to *B. bassiana* and *M. anisopliae*. Full statistical details are available on Table S8. Related to Figure 5.

Figure S6. Fungal dissemination from wild-type and spz^{rm7} cadavers after natural infection with *M. anisopliae*. *Metarhizium anisopliae* extruding from cuticle and growing in spz^{rm7} cadavers are faster than that in wild-type cadavers. *M. anisopliae* can eventually disseminate through the whole flies both in wild-type and spz^{rm7} cadavers. Related to Figure 6.

Figure S7. Sum survival curves of single and compound host defense peptides mutants after infection with *B. bassiana*, *M. anisopliae*, *M. rileyi* and *E. muscae*. Full statistical details are available on Table S8. Related to Figure 7.

Figure S8. Sum survival curves of mutants of SPs involved in melanization after infection with *B. bassiana*, *M. anisopliae*, *M. rileyi* and *E. muscae*. Full statistical details are available on Table S8. Related to Figure 7.

Figure S9. Expression of *Drosomycin* of mutants of SPs involved in melanization upon natural and septic infection with *B. bassiana* and *M. anisopliae*. (**A-B**) Statistical analysis reveals higher *Drosomycin* expression in *PPO1, PPO2* double

1285 mutant compared to wild-type at 72 h and 120 h after natural infection with *B. bassiana*
1286 and at 72 h after natural infection with *M. anisopliae* (*, P<0.05; ***, P<0.001). The
1287 spz^{rm7} flies as a positive control. (**C**) Compared with wild-type flies, PPO1, PPO2
1288 double mutant flies exhibit an enhanced Toll pathway activity upon clean injury and
1289 septic infection with *M. anisopliae* (ns, P>0.05; *, p<0.05; ***, P<0.001; ****,
1290 P<0.0001). Expression was normalized with w^{1118} UC set as a value of 1. Data were
1291 analyzed using One-Way ANOVA followed by Tukey's multiple comparison tests and
1292 values represent the mean ± s.d. of at least three independent experiments. Full
1293 statistical details are available on Table S8. Related to Figure 7.

Figure 1

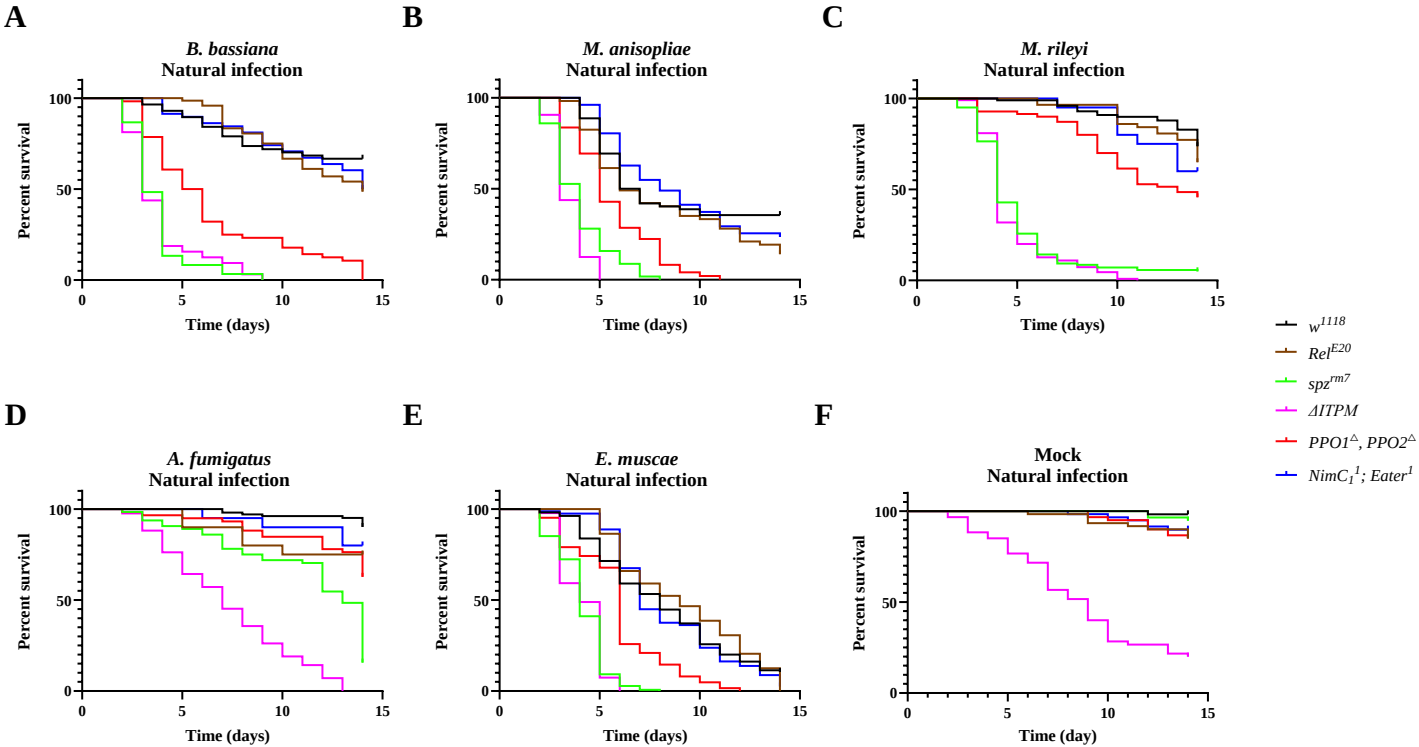
A
B. bassiana
Natural infection
B
M. anisopliae
Natural infection
C
M. rileyi
Natural infection
D
A. fumigatus
Natural infection
E
E. muscae
Natural infection
F
Mock
Natural infection
Percent survival
Time (days)
Time (day)
0
50
100
0
5
10
15
w1118
Rel E20
spz rm7
ΔITPM
PPO1Δ, PPO2Δ
NimC1 1; Eater1

Figure 2

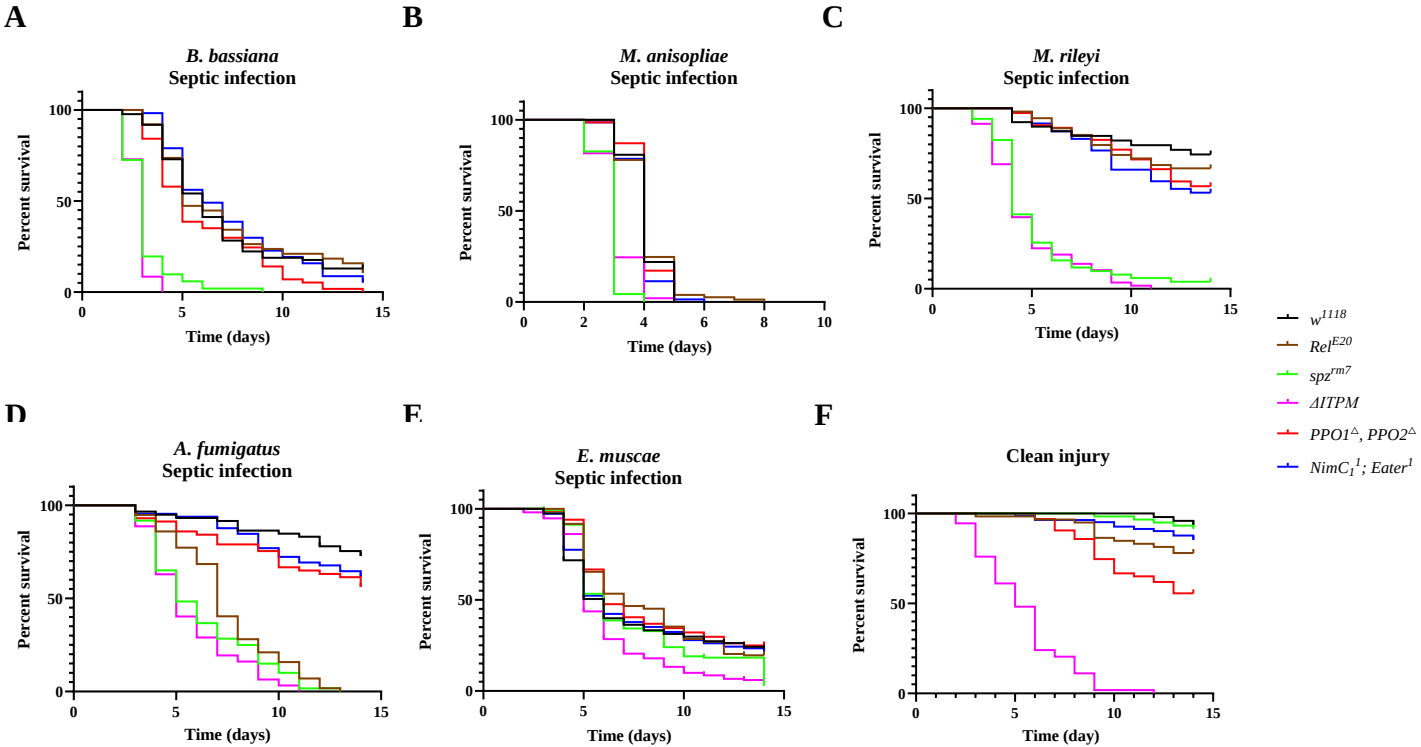
A
B. bassiana
Septic infection
Percent survival
Time (days)
B
M. anisopliae
Septic infection
Percent survival
Time (days)
C
M. rileyi
Septic infection
Percent survival
Time (days)
D
A. fumigatus
Septic infection
Percent survival
Time (days)
E
E. muscae
Septic infection
Percent survival
Time (days)
F
Clean injury
Percent survival
Time (day)
w1118
RelE20
spzrm7
ΔITPM
PPO1Δ, PPO2Δ
NimC1 1; Eater1

Figure 3

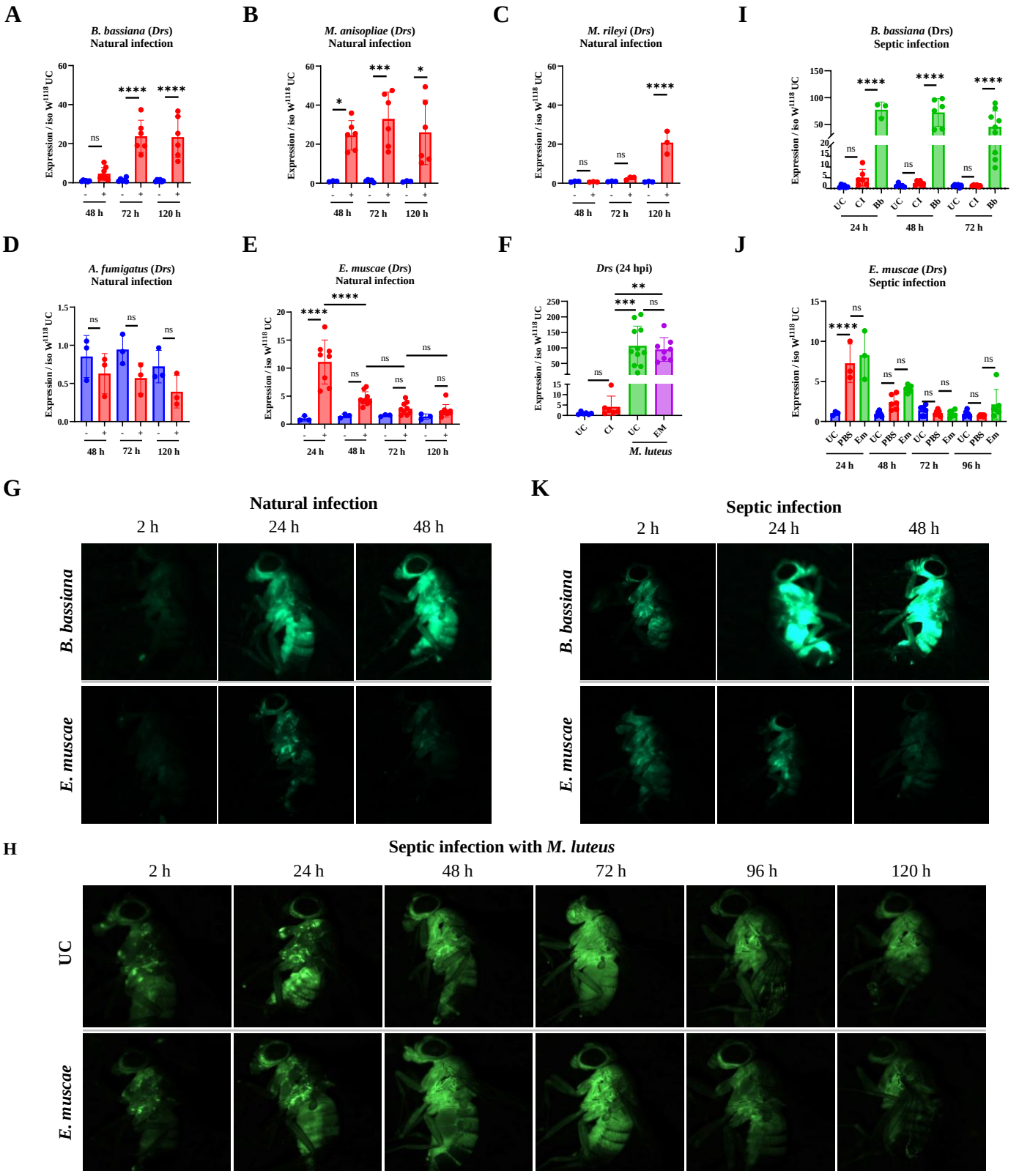
A
B. bassiana (Drs)
Natural infection
Expression / iso w1118 UC
48 h
72 h
120 h
B
M. anisopliae (Drs)
Natural infection
C
M. rileyi (Drs)
Natural infection
I
B. bassiana (Drs)
Septic infection
UC
Cl
Bb
24 h
48 h
72 h
D
A. fumigatus (Drs)
Natural infection
E
E. muscae (Drs)
Natural infection
F
Drs (24 hpi)
M. luteus
J
E. muscae (Drs)
Septic infection
PBS
Em
96 h
G
Natural infection
2 h
24 h
48 h
B. bassiana
E. muscae
K
Septic infection
H
Septic infection with M. luteus
72 h
96 h
120 h
UC

Figure 4

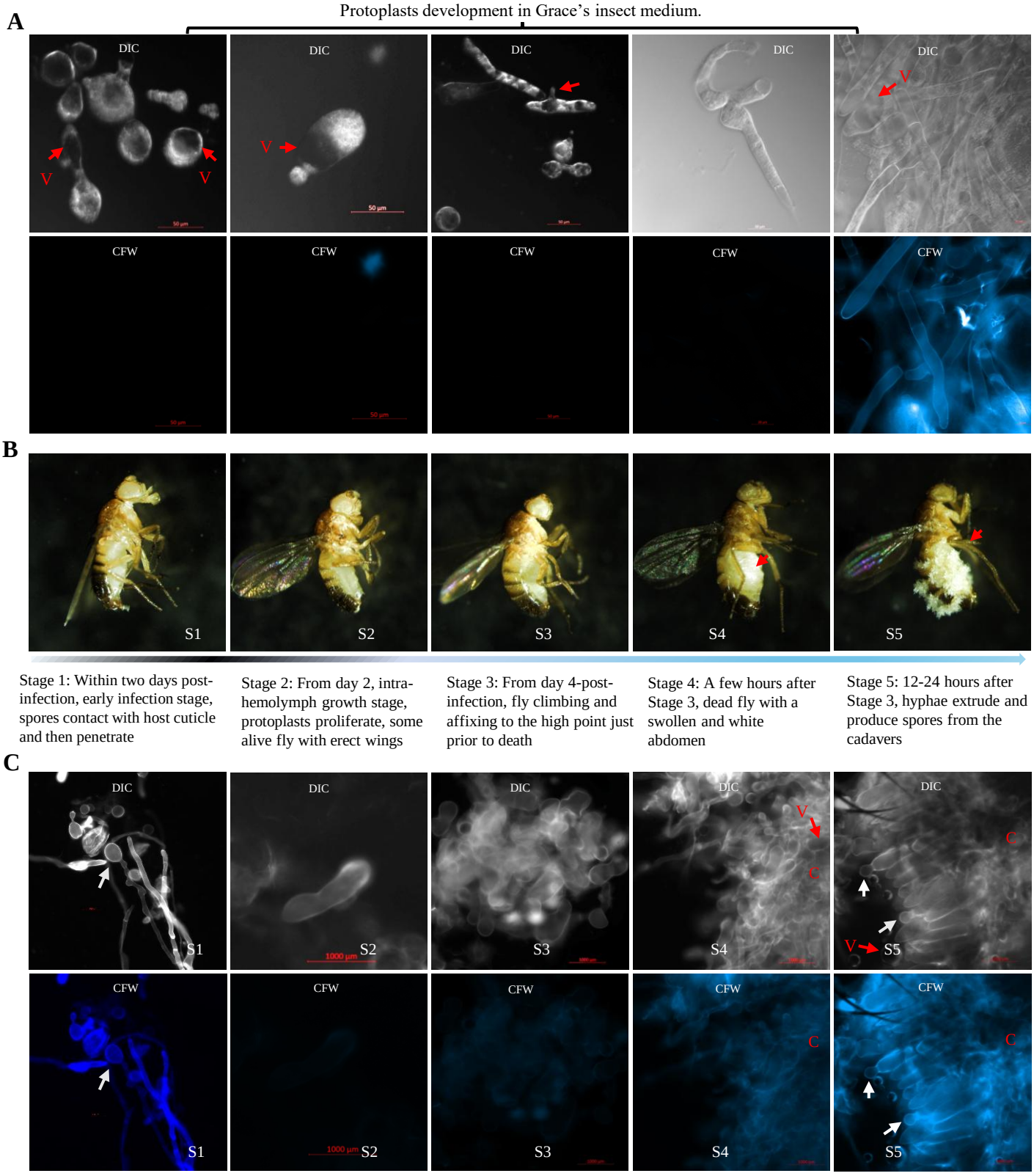
A
Protoplasts development in Grace's insect medium.
DIC
V
CFW
B
S1
S2
S3
S4
S5
Stage 1: Within two days post-infection, early infection stage, spores contact with host cuticle and then penetrate
Stage 2: From day 2, intra-hemolymph growth stage, protoplasts proliferate, some alive fly with erect wings
Stage 3: From day 4-post-infection, fly climbing and affixing to the high point just prior to death
Stage 4: A few hours after Stage 3, dead fly with a swollen and white abdomen
Stage 5: 12-24 hours after Stage 3, hyphae extrude and produce spores from the cadavers
C
C
1000 μm

Figure 5

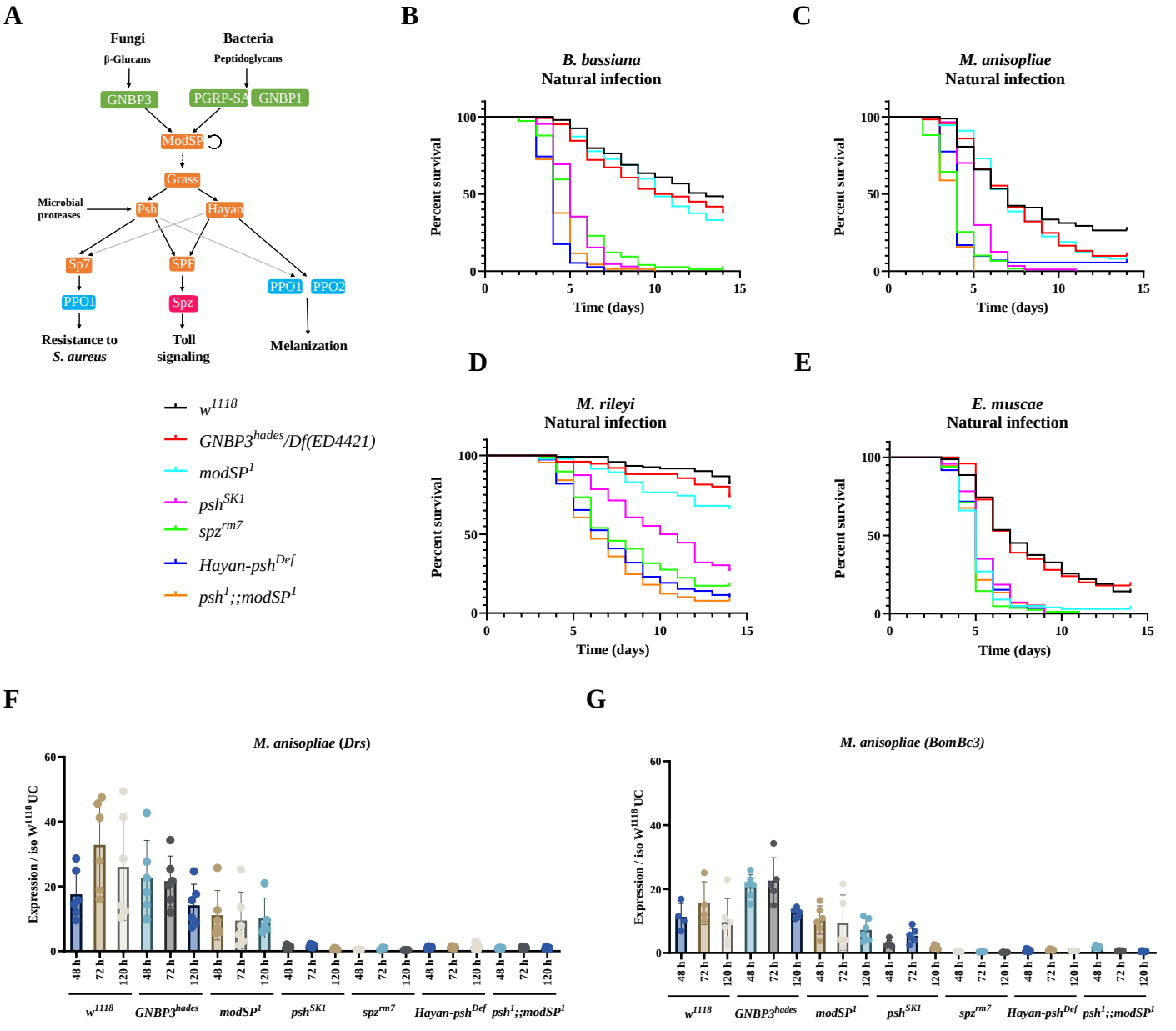
A
Fungi
Bacteria
β-Glucans
Peptidoglycans
GNBP3
PGRP-SA
GNBP1
ModSP
Grass
Microbial proteases
Psh
Hayan
Sp7
SPE
PPO1
PPO2
PPO1
Spz
Resistance to S. aureus
Toll signaling
Melanization
w1118
GNBP3hades/Df(ED4421)
modSP1
pshSK1
spzrm7
Hayan-pshDef
psh1;;modSP1
B
B. bassiana
Natural infection
Percent survival
Time (days)
C
M. anisopliae
Natural infection
D
M. rileyi
Natural infection
E
E. muscae
Natural infection
F
M. anisopliae (Drs)
Expression / iso w1118 UC
48 h
72 h
120 h
w1118
GNBP3hades
modSP1
pshSK1
spzrm7
Hayan-pshDef
psh1;;modSP1
G
M. anisopliae (BomBc3)

Figure 6

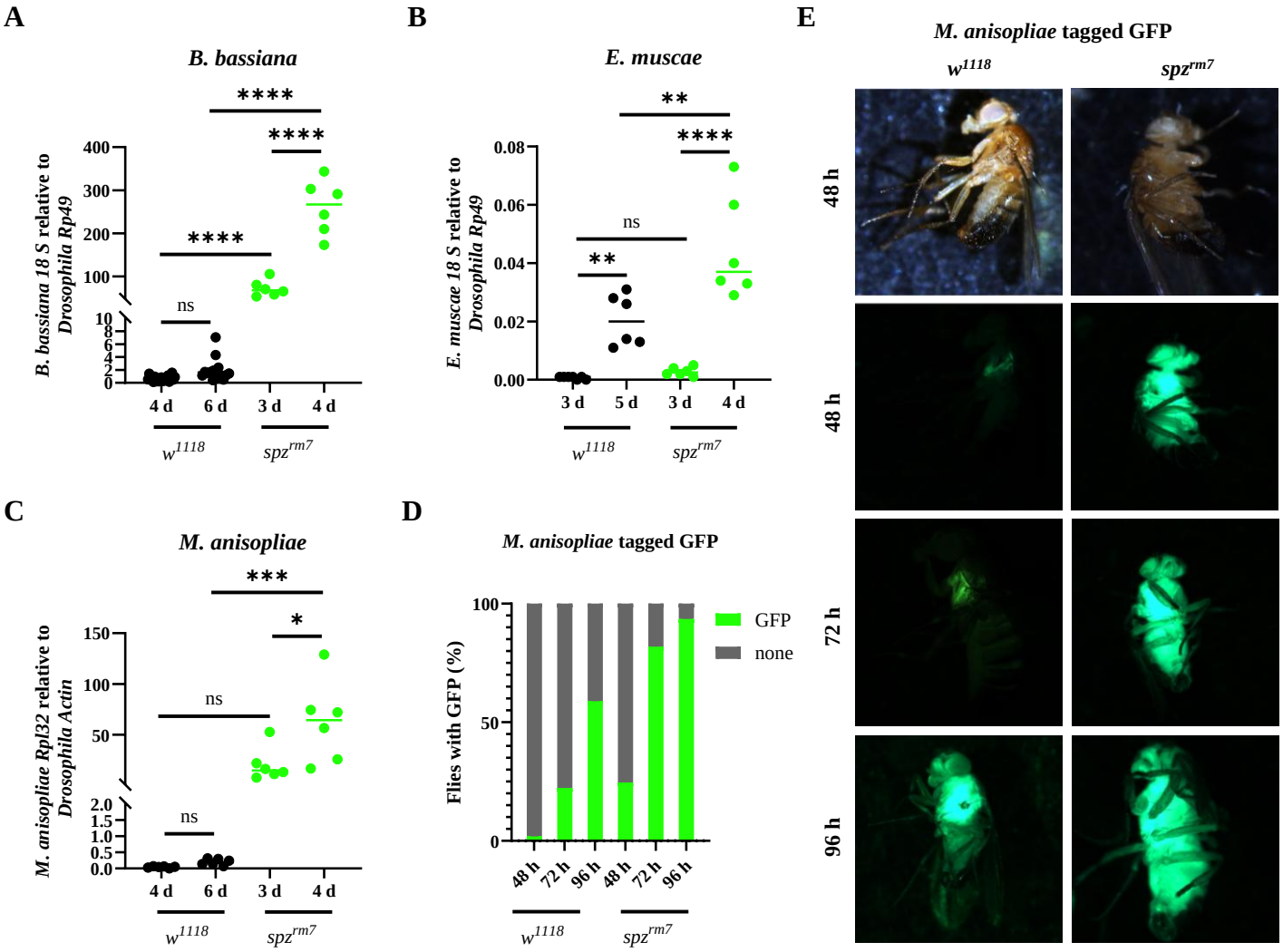
A
B. bassiana
B. bassiana 18 S relative to Drosophila Rp49
400
300
200
100
10
8
6
4
2
0
****
****
****
ns
4 d
6 d
3 d
4 d
w1118
spzrm7
B
E. muscae
E. muscae 18 S relative to Drosophila Rp49
0.08
0.06
0.04
0.02
0.00
**
****
ns
**
3 d
5 d
3 d
4 d
w1118
spzrm7
C
M. anisopliae
M. anisopliae Rpl32 relative to Drosophila Actin
150
100
50
2.0
1.5
1.0
0.5
0.0
***
*
ns
ns
4 d
6 d
3 d
4 d
w1118
spzrm7
D
M. anisopliae tagged GFP
Flies with GFP (%)
100
50
0
GFP
none
48 h
72 h
96 h
48 h
72 h
96 h
w1118
spzrm7
E
M. anisopliae tagged GFP
w1118
spzrm7
48 h
48 h
72 h
96 h

Figure 7

A

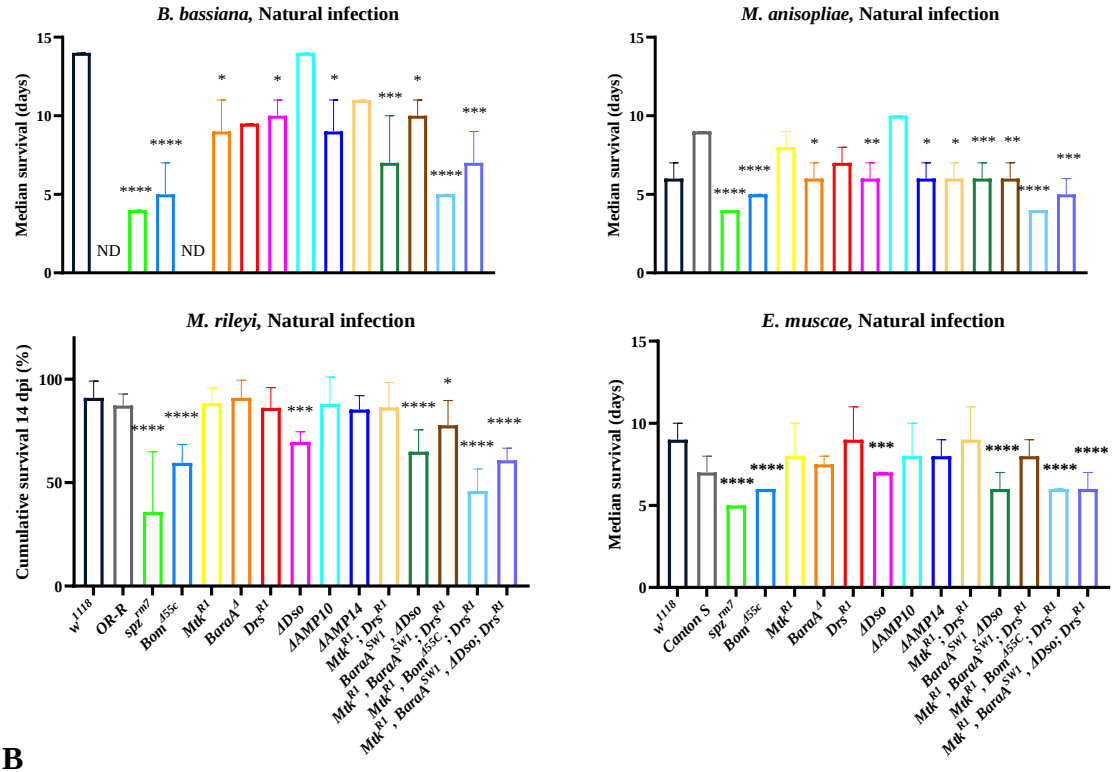
B. bassiana, Natural infection
M. anisopliae, Natural infection
M. rileyi, Natural infection
E. muscae, Natural infection
Median survival (days)
Cumulative survival 14 dpi (%)
ND
w1118
OR-R
spz rm7
Bom 455c
Mtk R1
BaraA 4
Drs R1
ΔDso
ΔAMP10
ΔAMP14
Mtk R1, Drs R1
BaraA SW1, Drs R1
Mtk R1, BaraA SW1
Mtk R1, Bom 455C, Drs R1
Mtk R1, BaraA SW1, ΔDso; Drs R1
Canton S

B

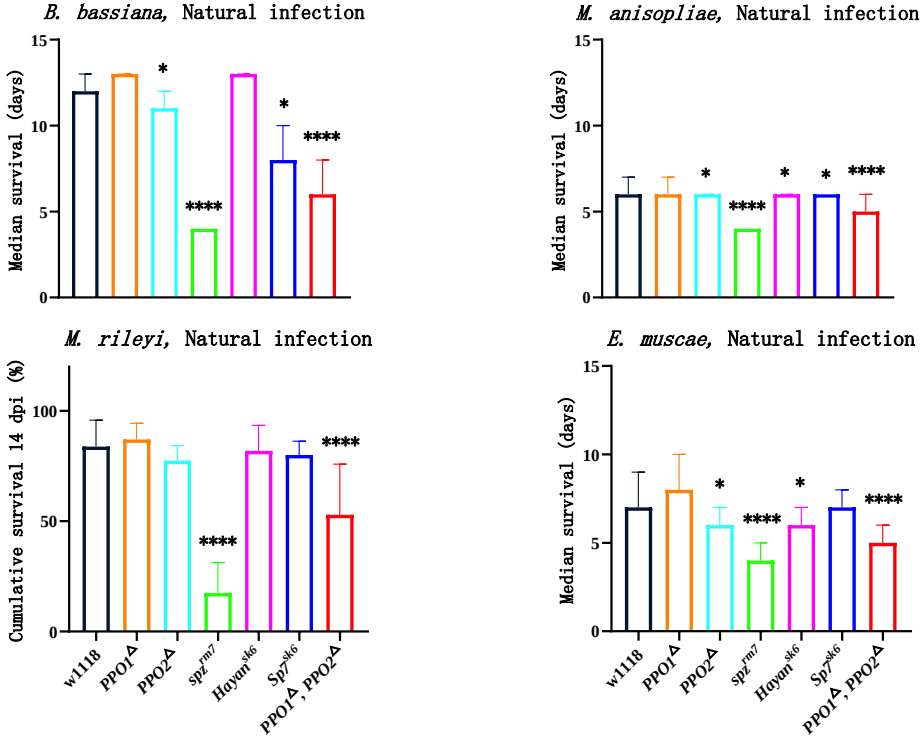
B. bassiana, Natural infection
M. anisopliae, Natural infection
M. rileyi, Natural infection
E. muscae, Natural infection
Median survival (days)
Cumulative survival 14 dpi (%)
w1118
PPO1Δ
PPO2Δ
spz rm7
Hayan sk6
Spz sk6
PPO1Δ, PPO2Δ

Figure 8

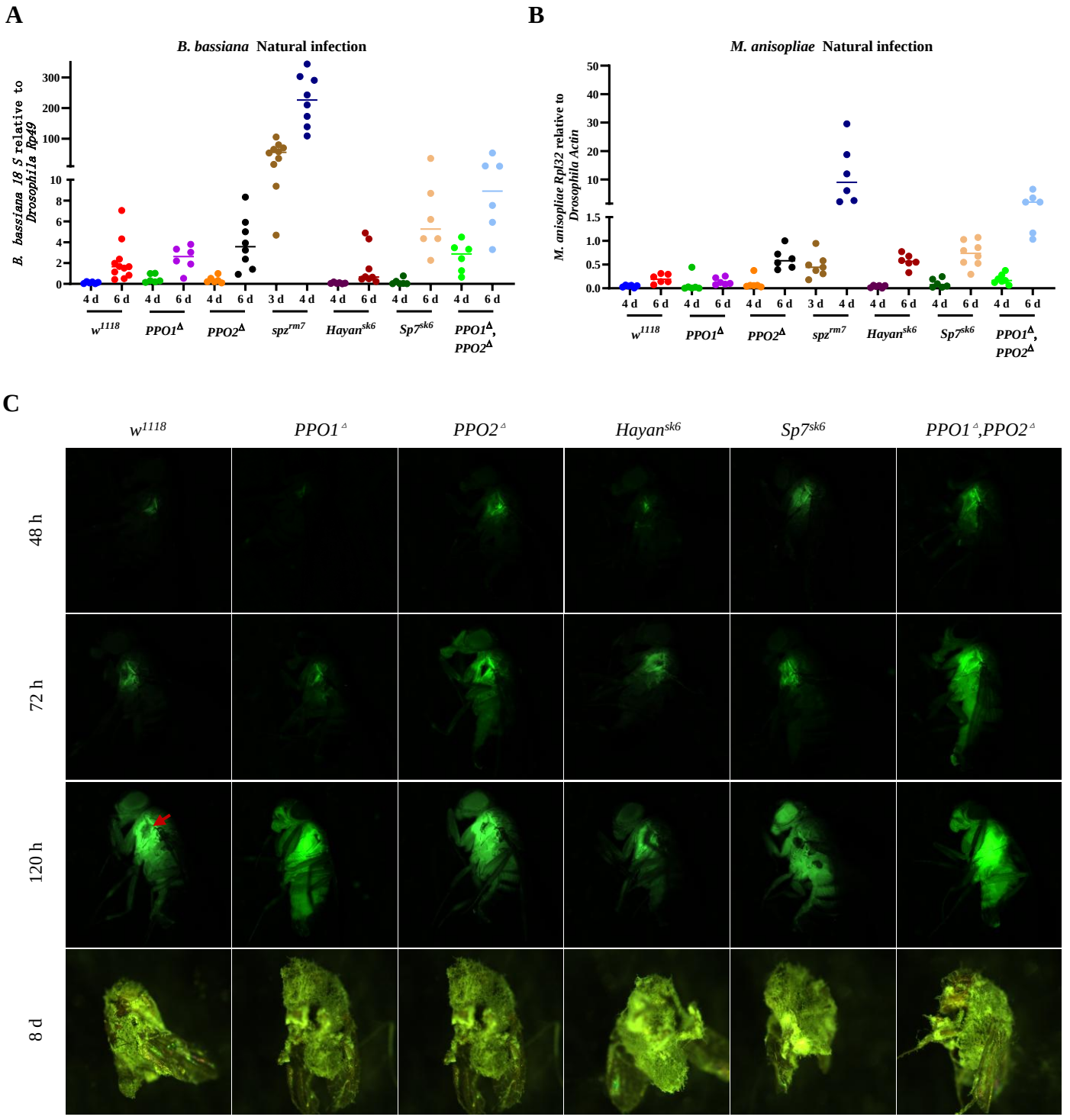
A
B. bassiana Natural infection
B. bassiana 18 S relative to Drosophila Rp49
300
200
100
10
8
6
4
2
0
4 d
6 d
3 d
w1118
PPO1Δ
PPO2Δ
spzrm7
Hayansk6
Sp7sk6
PPO1Δ, PPO2Δ
B
M. anisopliae Natural infection
M. anisopliae Rpl32 relative to Drosophila Actin
50
40
30
20
10
1.5
1.0
0.5
0.0
C
w1118
PPO1Δ
PPO2Δ
Hayansk6
Sp7sk6
PPO1Δ,PPO2Δ
48 h
72 h
120 h
8 d

Figure S1

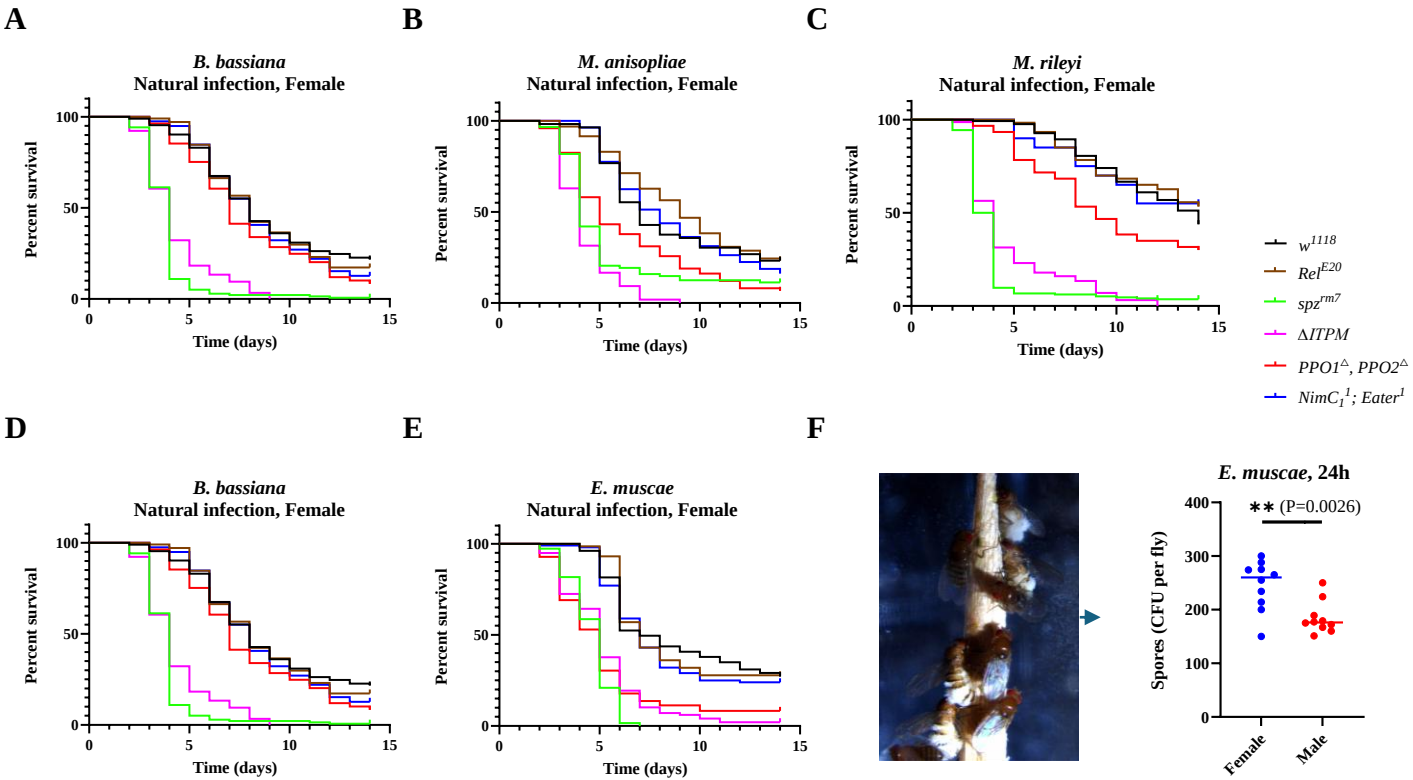
A
B. bassiana
Natural infection, Female
Percent survival
Time (days)
B
M. anisopliae
Natural infection, Female
Percent survival
Time (days)
C
M. rileyi
Natural infection, Female
Percent survival
Time (days)
w1118
Rel E20
spz rm7
ΔITPM
PPO1Δ, PPO2Δ
NimC1 1; Eater1
D
B. bassiana
Natural infection, Female
Percent survival
Time (days)
E
E. muscae
Natural infection, Female
Percent survival
Time (days)
F
E. muscae, 24h
** (P=0.0026)
Spores (CFU per fly)
Female
Male

Figure S2

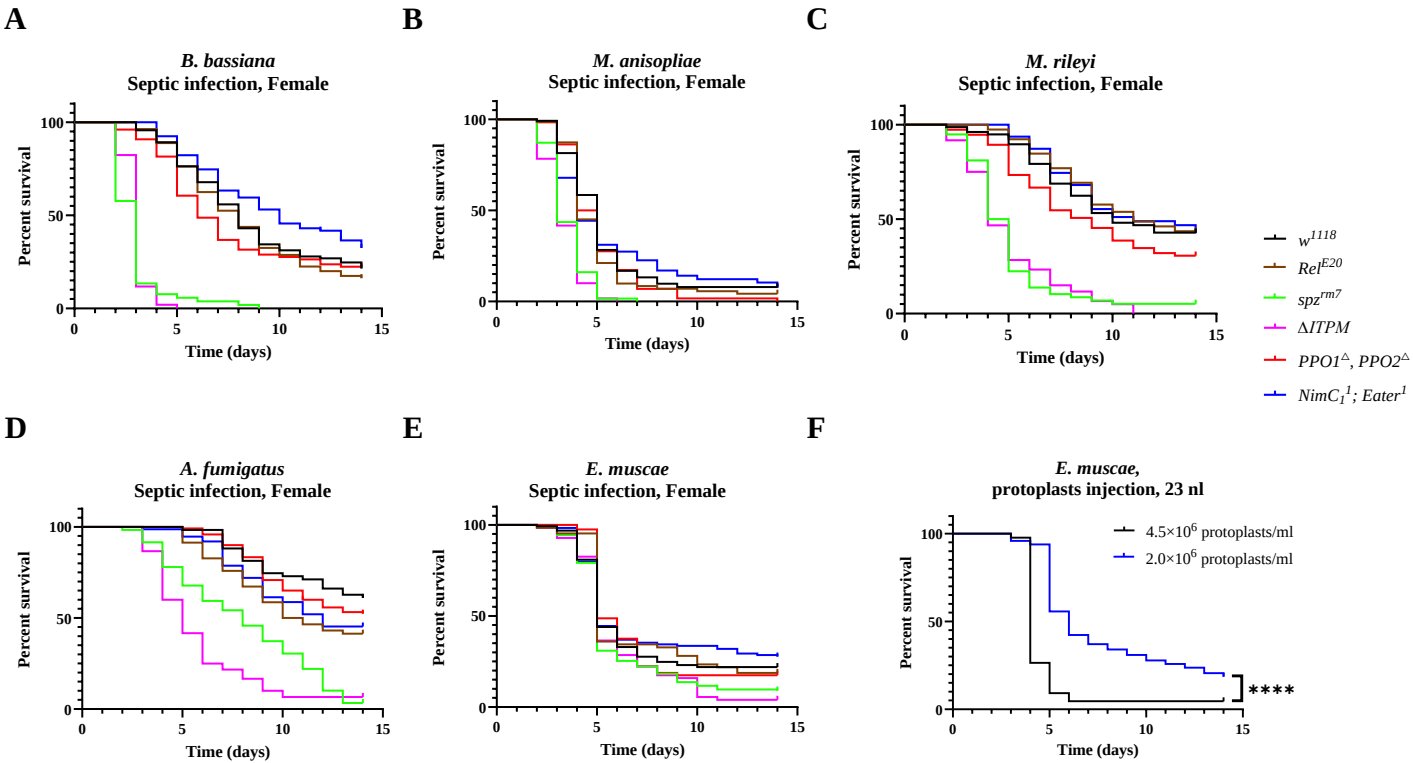
A
B. bassiana
Septic infection, Female
B
M. anisopliae
Septic infection, Female
C
M. rileyi
Septic infection, Female
D
A. fumigatus
Septic infection, Female
E
E. muscae
Septic infection, Female
F
E. muscae,
protoplasts injection, 23 nl
Percent survival
Time (days)
0
50
100
0
5
10
15
w1118
RelE20
spzrm7
ΔITPM
PPO1Δ, PPO2Δ
NimC1 1; Eater1
4.5×10^6 protoplasts/ml
2.0×10^6 protoplasts/ml
****

Figure S3

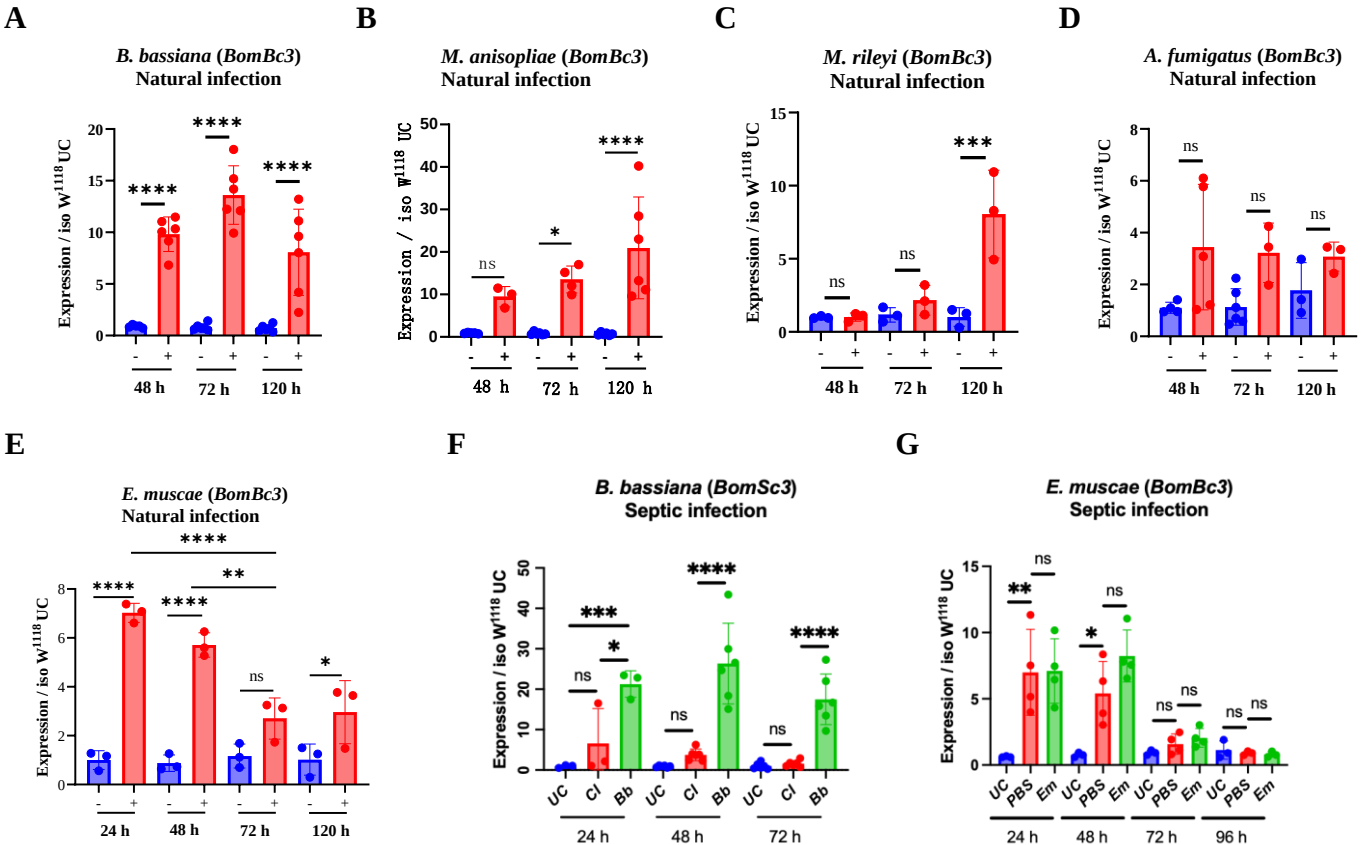
A
B. bassiana (BomBc3)
Natural infection
Expression / iso W1118 UC
48 h
72 h
120 h
B
M. anisopliae (BomBc3)
Natural infection
Expression / iso W1118 UC
C
M. rileyi (BomBc3)
Natural infection
Expression / iso W1118 UC
D
A. fumigatus (BomBc3)
Natural infection
Expression / iso W1118 UC
E
E. muscae (BomBc3)
Natural infection
Expression / iso W1118 UC
24 h
F
B. bassiana (BomSc3)
Septic infection
Expression / iso W1118 UC
UC
CI
Bb
G
E. muscae (BomBc3)
Septic infection
Expression / iso W1118 UC
PBS
Em
96 h

Figure S4

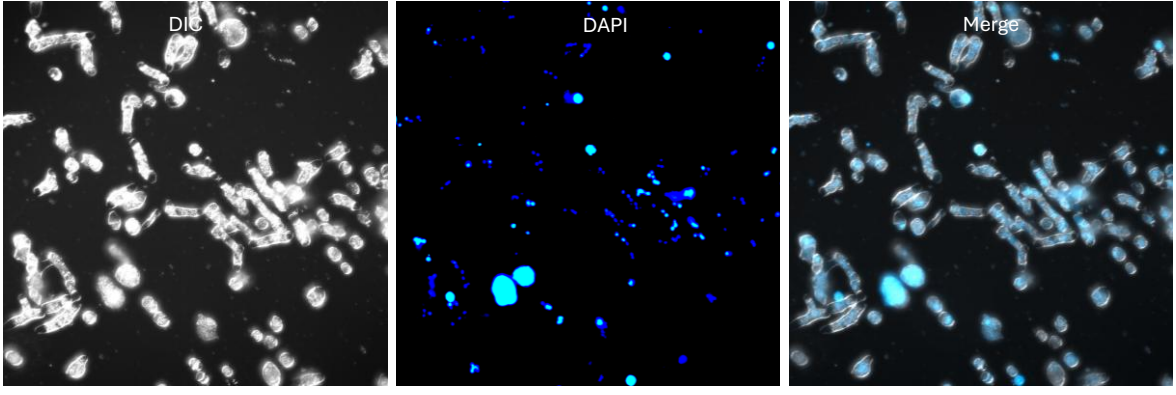

Figure S5

A

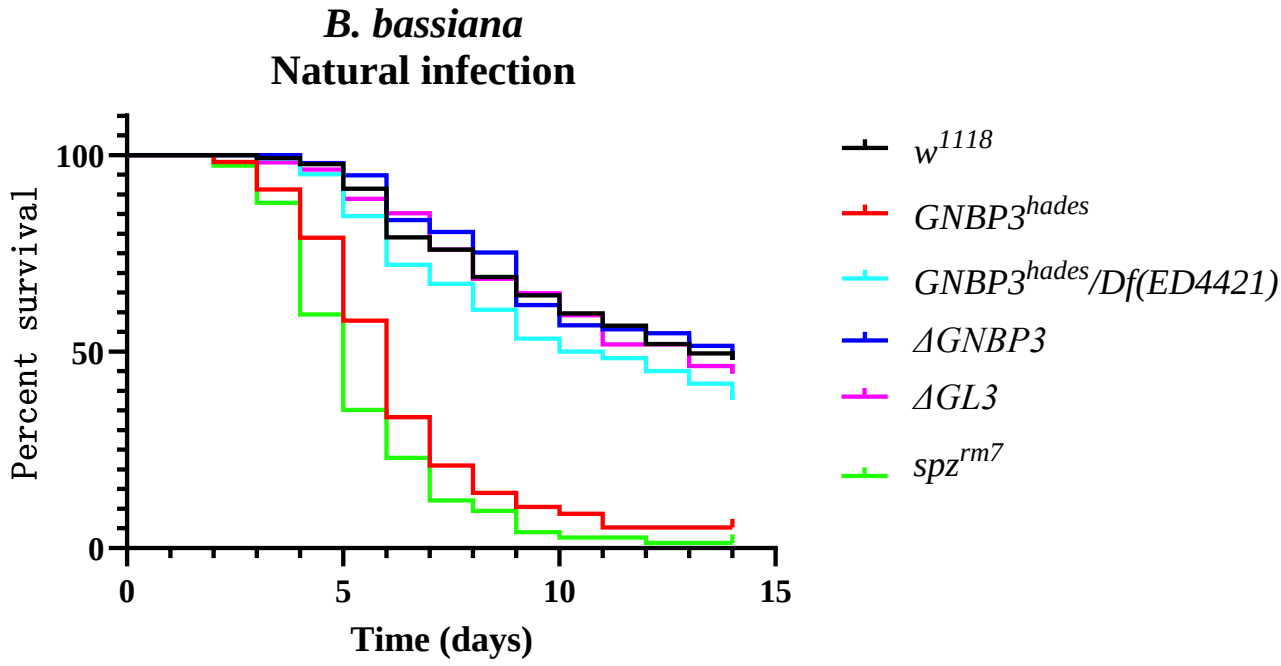
B. bassiana
Natural infection
Percent survival
100
50
0
0
5
10
15
Time (days)
w1118
GNBP3hades
GNBP3hades/Df(ED4421)
ΔGNBP3
ΔGL3
spzrm7

B

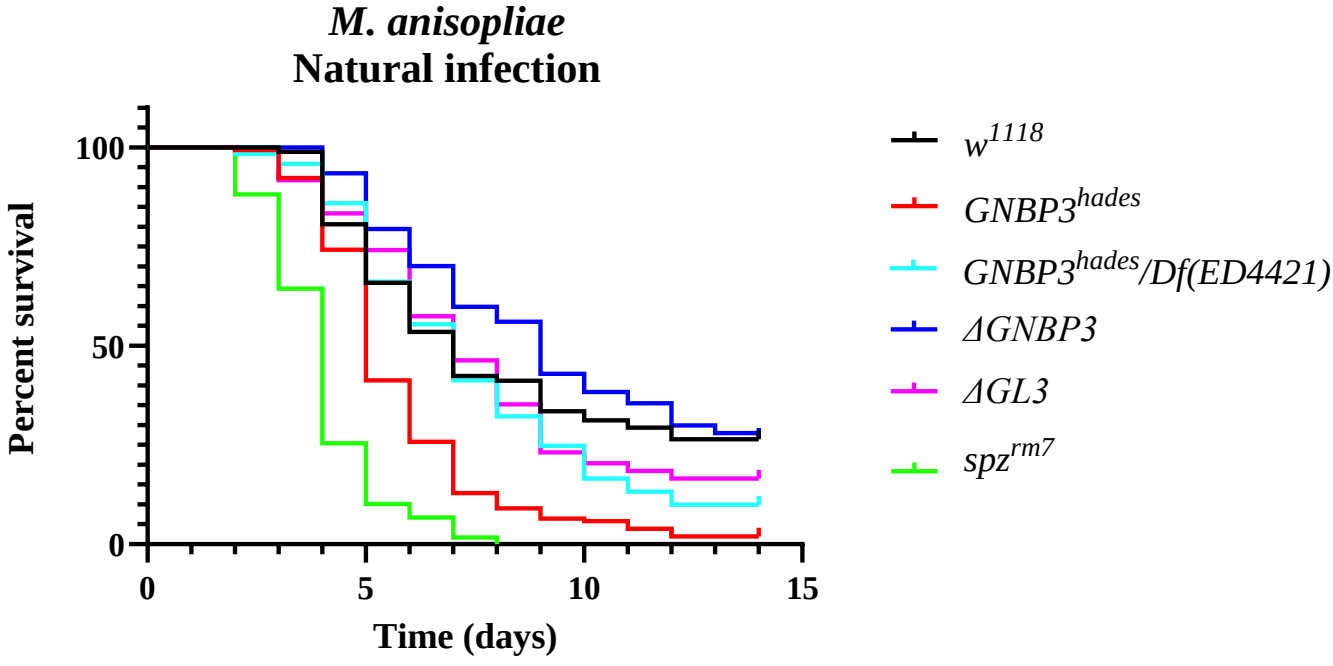
M. anisopliae
Natural infection
Percent survival
100
50
0
0
5
10
15
Time (days)
w1118
GNBP3hades
GNBP3hades/Df(ED4421)
ΔGNBP3
ΔGL3
spzrm7

Figure S6

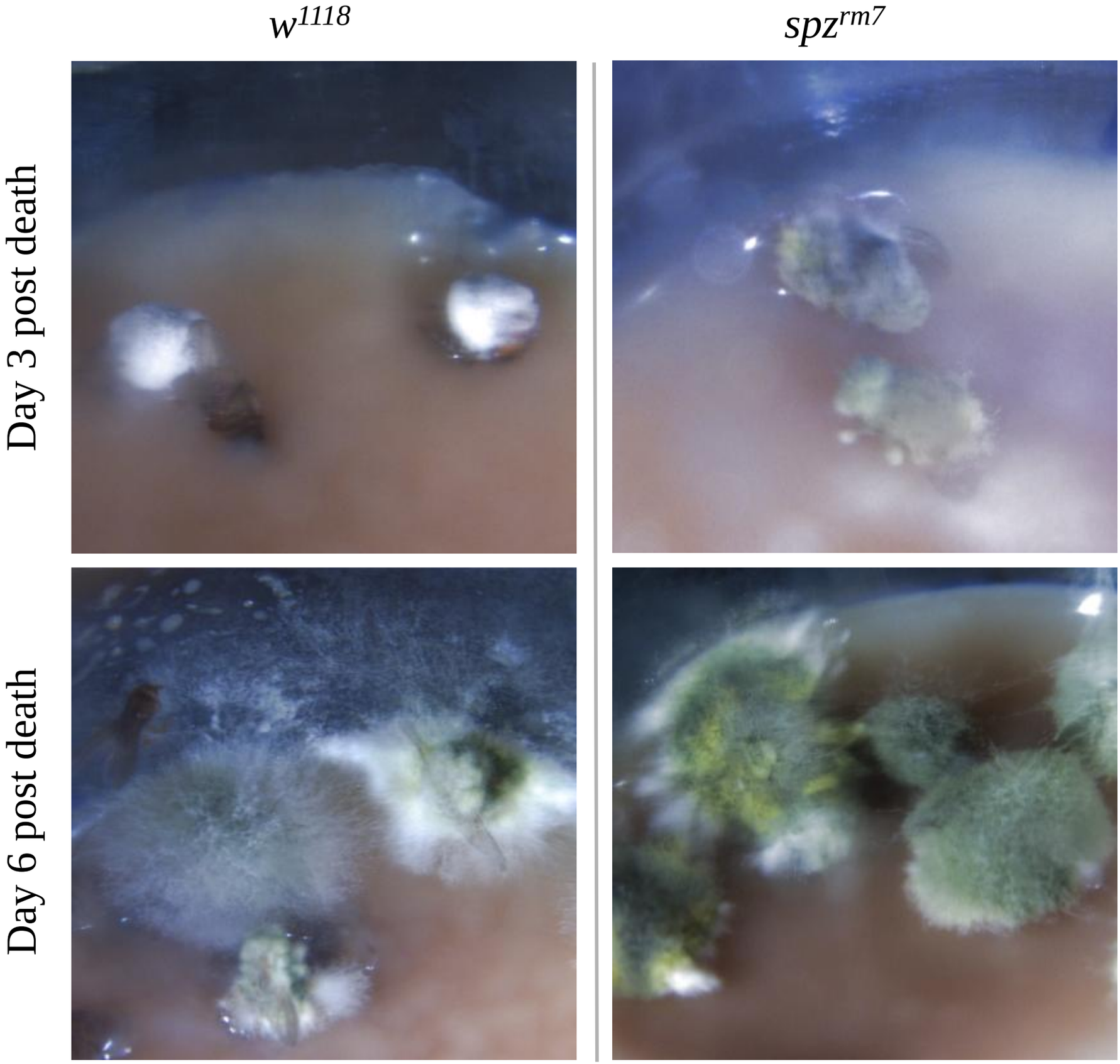

Figure S7

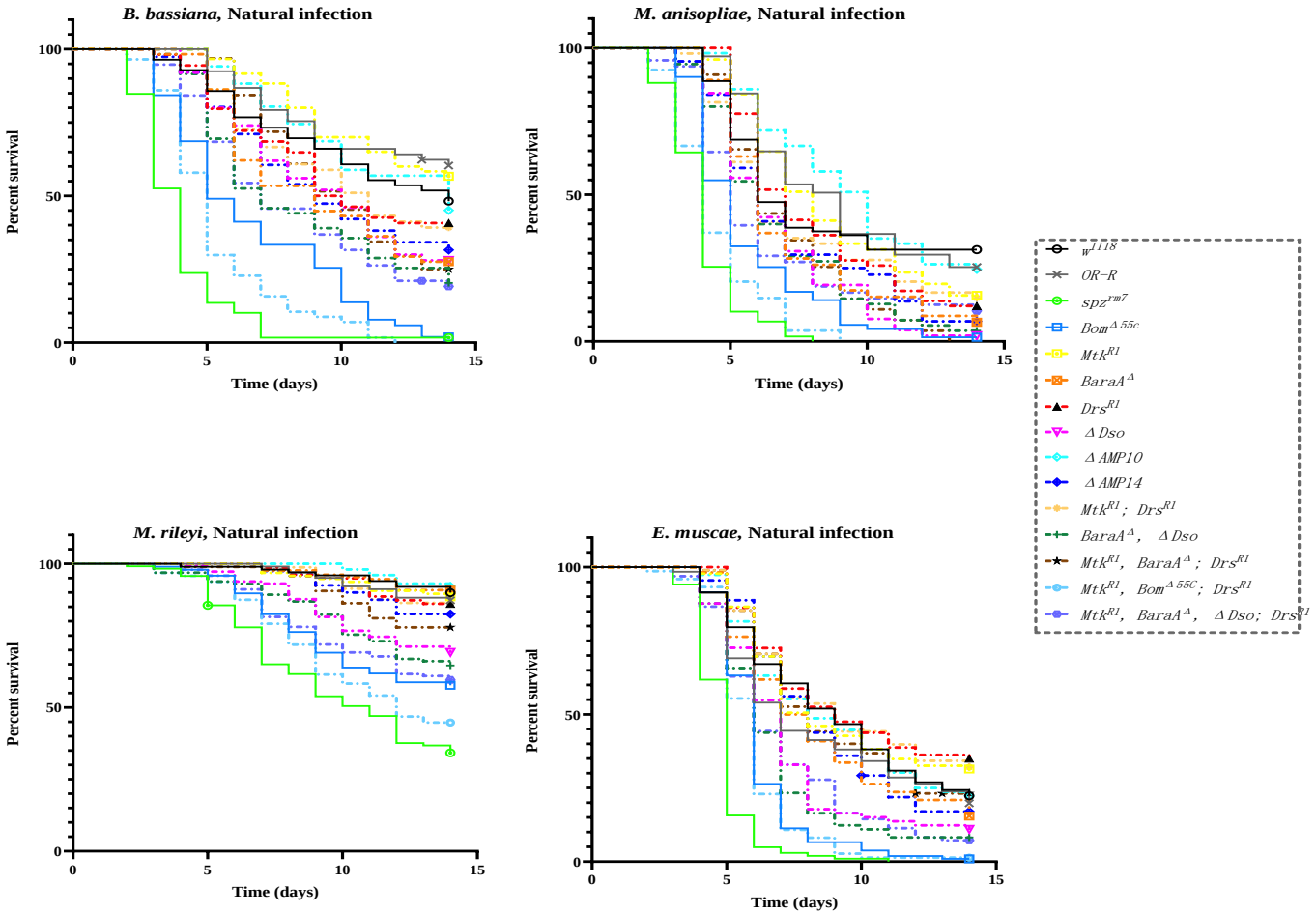
B. bassiana, Natural infection
M. anisopliae, Natural infection
M. rileyi, Natural infection
E. muscae, Natural infection
Percent survival
Time (days)
0
50
100
0
5
10
15
w1118
OR-R
spzrm7
BomΔ55c
MtkR1
BaraAΔ
DrsR1
ΔDso
ΔAMP10
ΔAMP14
MtkR1; DrsR1
BaraAΔ, ΔDso
MtkR1, BaraAΔ; DrsR1
MtkR1, BomΔ55C; DrsR1
MtkR1, BaraAΔ, ΔDso; DrsR1

Figure S8

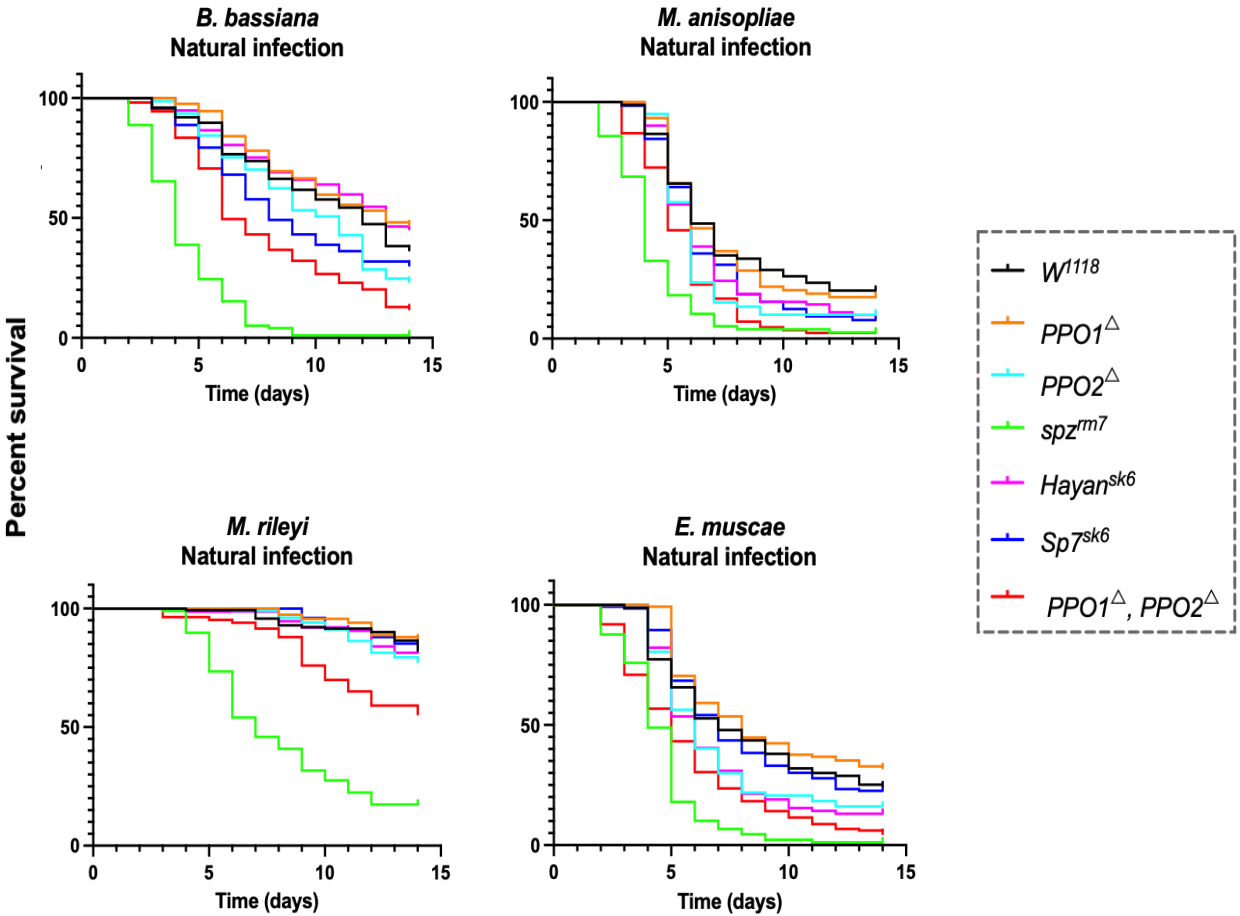
B. bassiana
Natural infection
M. anisopliae
Natural infection
M. rileyi
Natural infection
E. muscae
Natural infection
Percent survival
Time (days)
0
5
10
15
50
100
W1118
PPO1△
PPO2△
spzrm7
Hayansk6
Sp7sk6
PPO1△, PPO2△

Figure S9

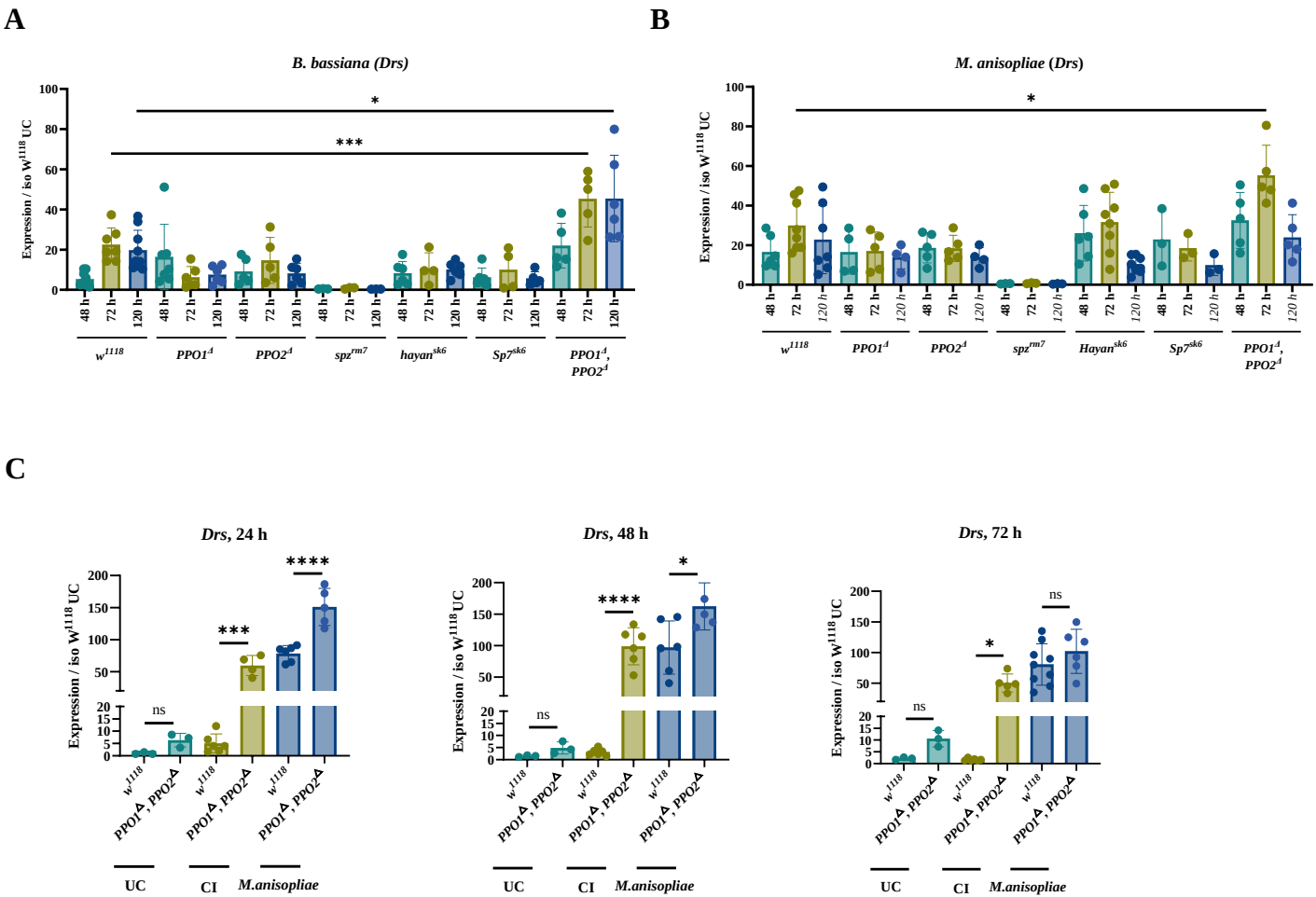
A
B. bassiana (Drs)
Expression / iso w1118 UC
*
***
48 h
72 h
120 h
w1118
PPO1Δ
PPO2Δ
spzrm7
hayansk6
Sp7sk6
PPO1Δ, PPO2Δ
B
M. anisopliae (Drs)
Expression / iso w1118 UC
*
Hayansk6
C
Drs, 24 h
Drs, 48 h
Drs, 72 h
Expression / iso w1118 UC
ns
*
***
****
w1118
PPO1Δ, PPO2Δ
UC
CI
M.anisopliae